SAND2018-7975C

Study of Galinstan Liquid Metal Breakup Using Backlit Imaging and Digital In-line Holography

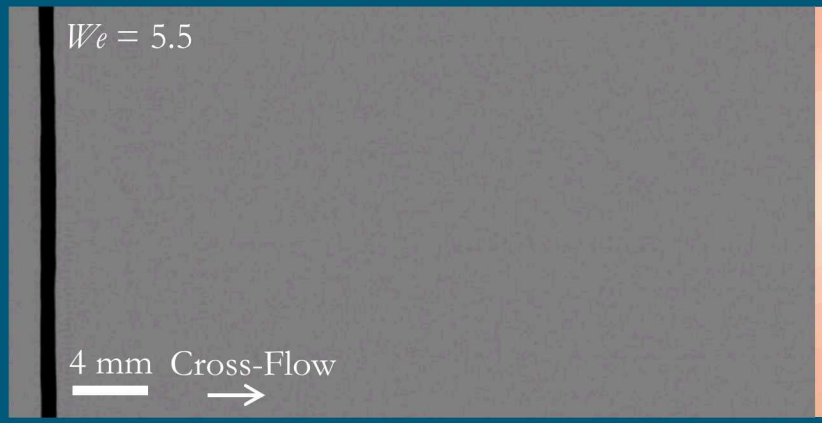

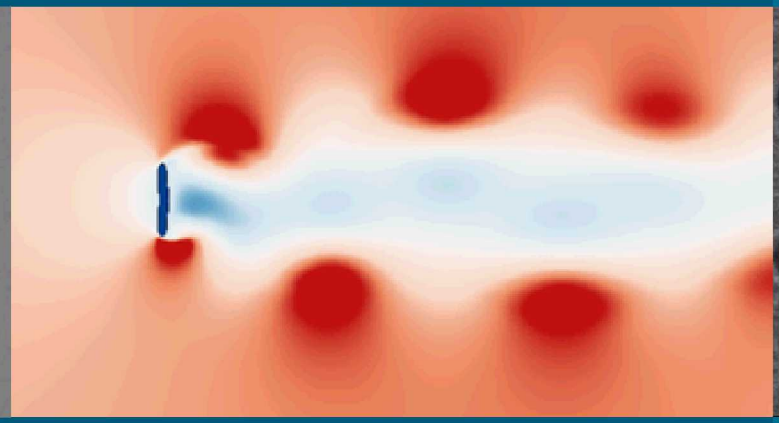

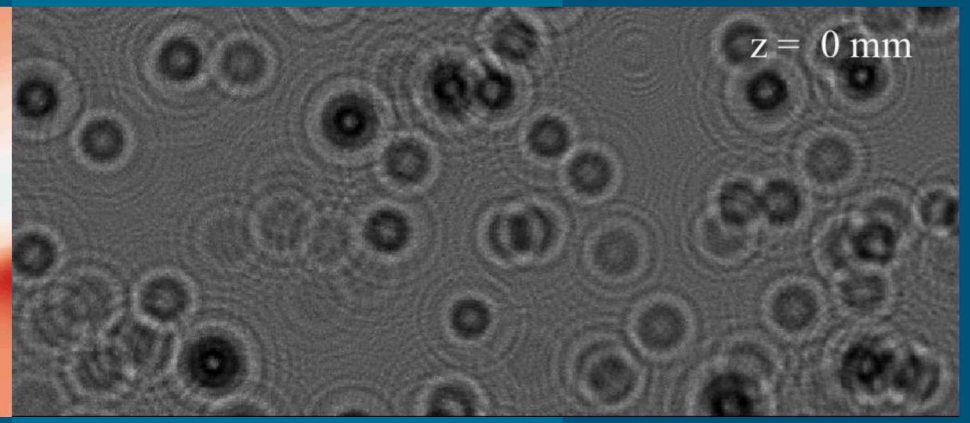

Ellen Yi Chen, Justin L. Wagner, Paul A. Farias, and Daniel R. Guildenbecher

International Conference on Liquid Atomization and Spray Systems, Chicago, Illinois, July 21nd-26th, 2018

Sandia National Laboratories is a multimission laboratory managed and operated by National Technology & Engineering Solutions of Sandia, LLC, a wholly owned subsidiary of Honeywell International Inc., for the U.S. Department of Energy's National Nuclear Security Administration under contract DE-NA0003525.

Motivation

- Why is the aerodynamic breakup of liquid metal important?
- Simulations suggest that liquid metal (high density ratio) breakup has more intensive fragmentation[1]
- Experimental investigations of liquid metal breakup in cross flows are limited[2]
- Breakup morphology as a function of Weber number and secondary droplet formation are important

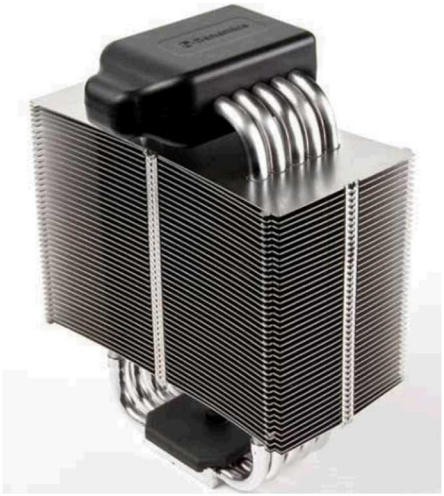

Liquid Metal Cooling Systems

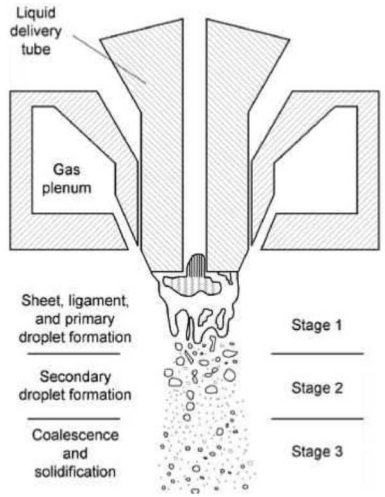

Metal Powder Formation

W.R. Lane, 1951

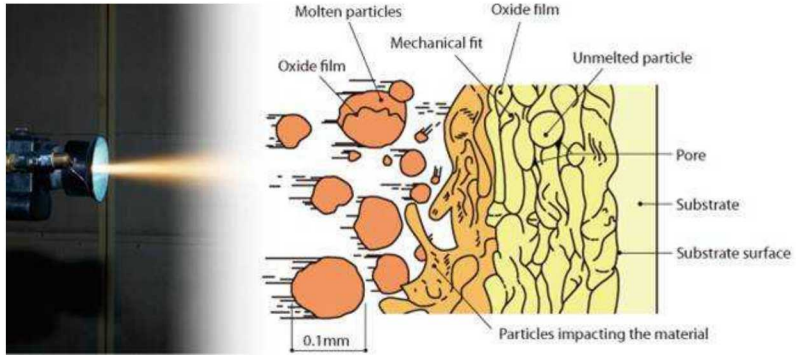

Thermal Spray Coatings

Model Validation

Y. Ling et al. 2013

Understanding Accident Scenarios

1. W. Yang et al. 2016
2. L.-P. Hsiang and G. M. Faeth 1994

Liquid Metal Breakup

- Breakup morphology and secondary droplet formation are important parameters which scale with non-dimensional numbers:

$$We = \frac{\rho_g u^2 d}{\sigma} \qquad \tau = \frac{tu}{d}\sqrt{\frac{\rho_g}{\rho_l}} = \frac{tu}{d}\frac{1}{\sqrt{\rho^*}}$$

- Column breakup transitions occur at slightly lower Weber numbers than spheres due to the capillary instability
- Liquid metals have unique characteristics such as high density, high surface tension, fast surface oxide formation
- Galinstan (68.5% gallium, 21.5% indium and 10% tin) is a non-toxic eutectic liquid metal at room temperature that forms a surface oxide
  - Melting temperature of -19 degrees Celsius
  - Forms passivating, elastic oxide layers (Ga2O3/Ga2O, surface yield stress of EGaIn is ~ 0.5 N/m) preventing the formation of perfectly spherical droplets

Properties	Galinstan	Water
Density	~ 6440 kg/m^3	~ 1000 kg/m^3
Surface Tension	~ 0.718 N/m	~ 0.073 N/m
Bulk Viscosity	~ 2.4 mPa·s	~ 0.89 mPa·s

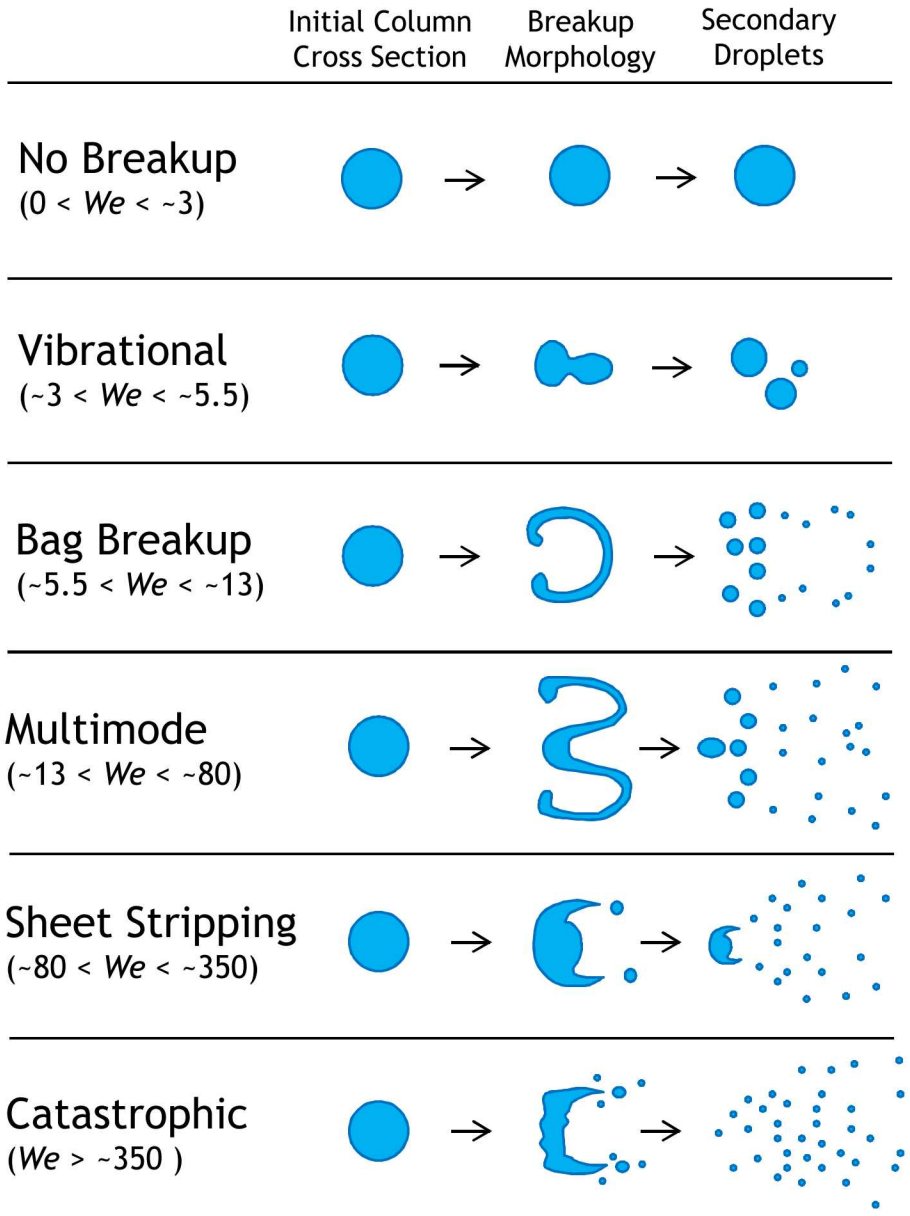

Experimental Setup

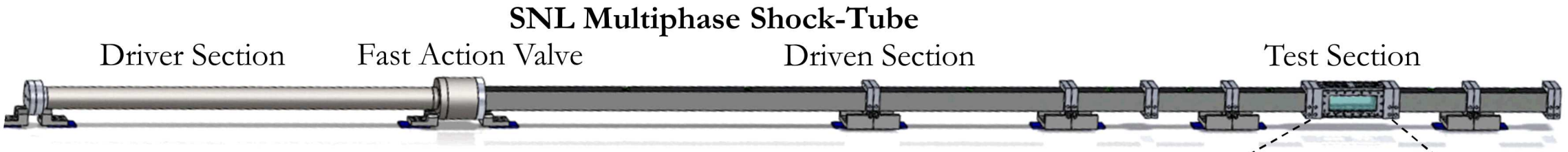

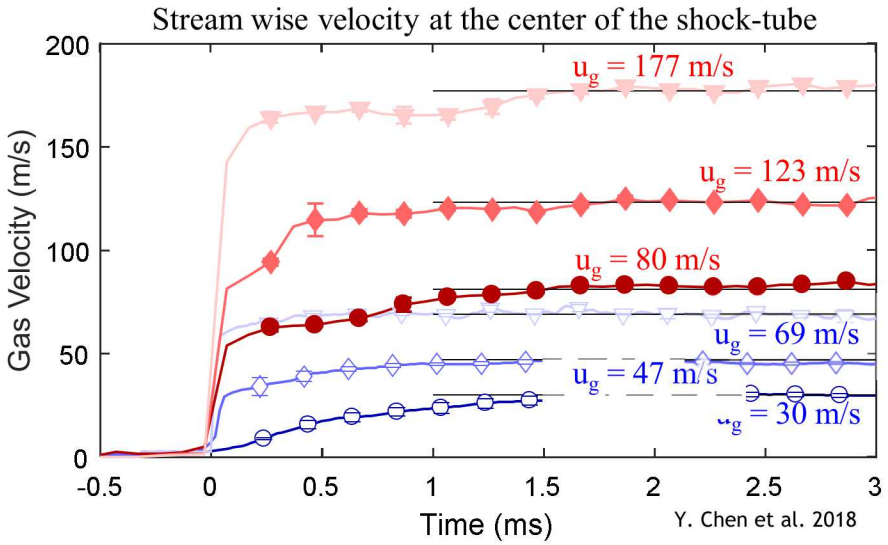

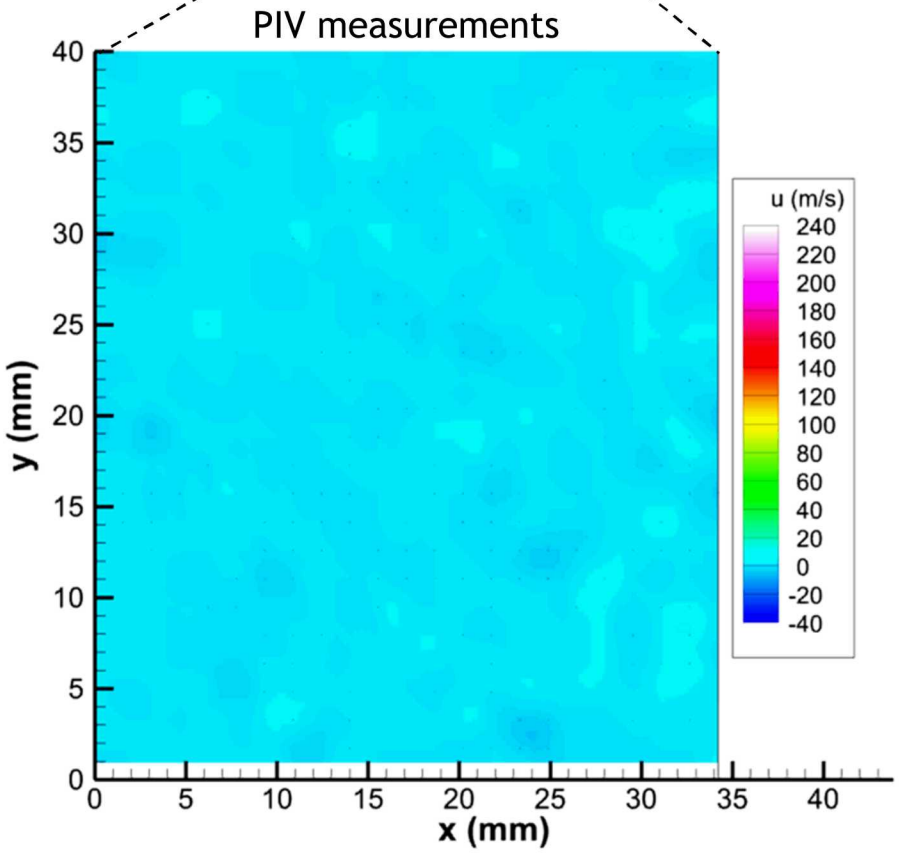

- 76 ×76 mm cross section and 5.2 m long
- Generates shock waves using pressurized nitrogen and a fast action valve
- Driven gas is air at 300K and 84.1 kPa (Albuquerque, NM)
- Provides a uniform step change in velocity (Mach 1 to 1.5, u_g = 30 to 177 m/s)
- Test times of 5 to 10 ms determined by the reflected shock time

Experimental Setup

SNL Multiphase Shock-Tube

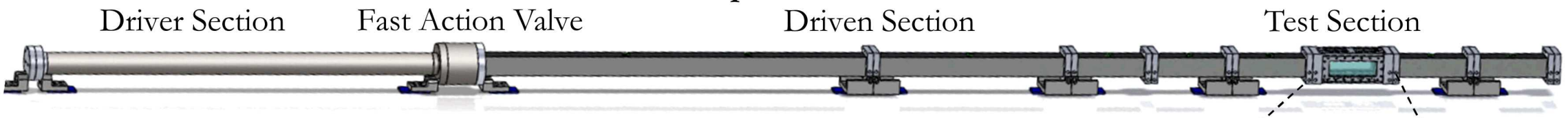

- A precision fluid dispensing system formed laminar jets using low liquid volumes (Nordson EFD Performus)
- Driven with pressurized air from 1-8 psig
- Column diameters d_c = 0.5 to 1.36 mm
- A liquid catch is used to prevent gas leakage
- Stainless steel test sections, Acrylic windows, and tape were used to prevent Galinstan from damaging the walls and wetting to the walls

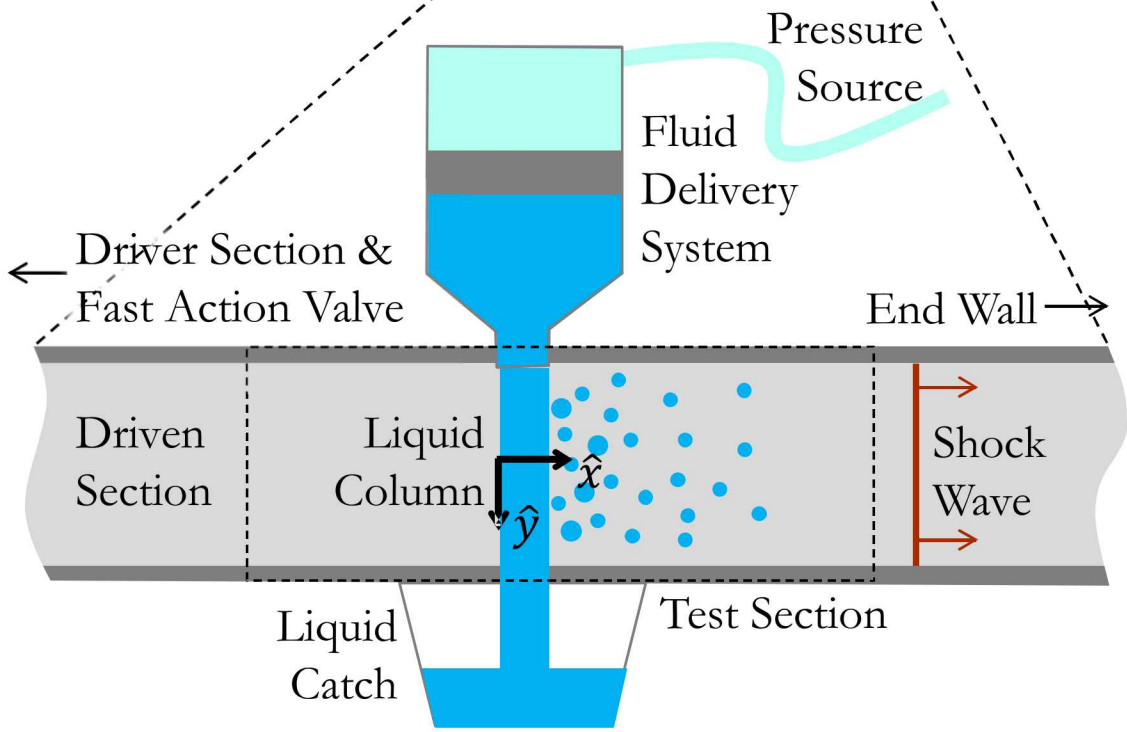

Side View - Fluid Delivery System

Experimental Setup

- Used an LED backlight and diffuser
- Two Photron SA-Z cameras (100 kHz)
- Perpendicular and oblique cameras was used to help classify morphology
- Column y-velocities were estimated (<3 m/s) and were found to be much less than the convective velocities used
- Technique is useful for qualitative assessment

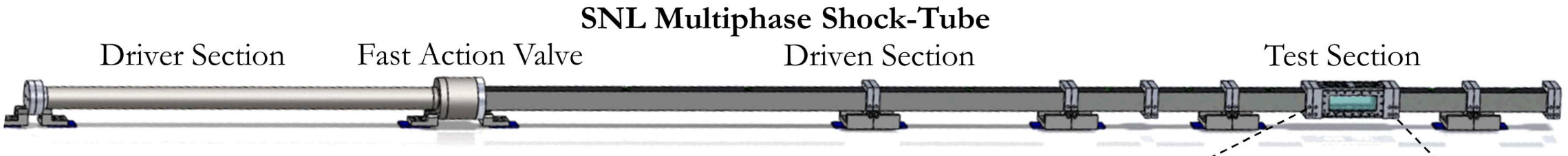

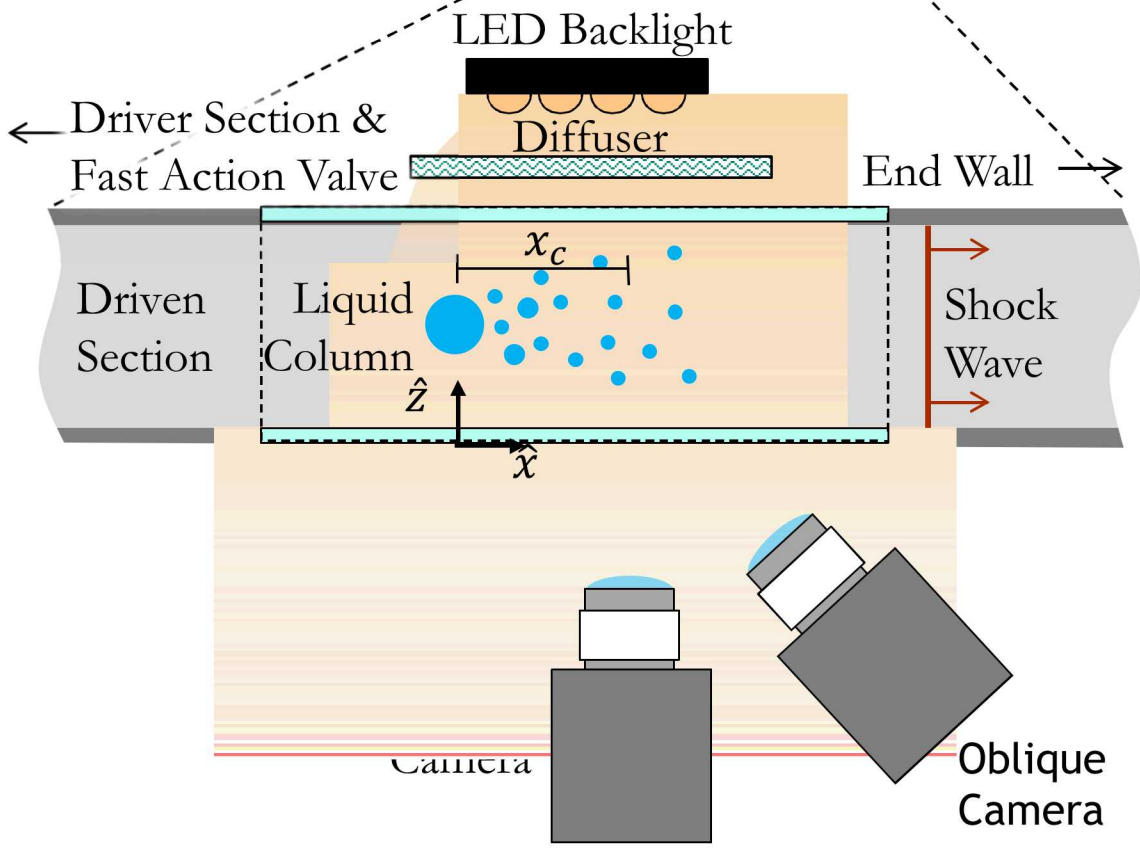

Top View – Backlit Imaging

Backlit Results

Bag Breakup

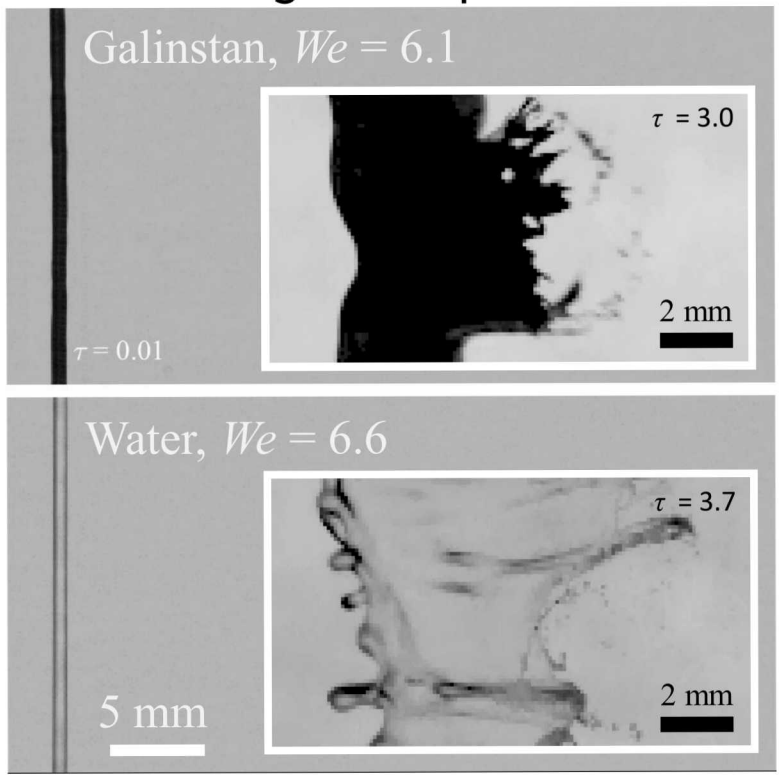

d = 0.84 mm
Galinstan Conditions: Ma = 1.41, u = 204.7 m/s, ρ_g = 1.67 kg/m^3
Water Conditions: Ma = 1.15, u = 80.0 m/s, ρ_g = 1.22 kg/m^3

Multimode Breakup

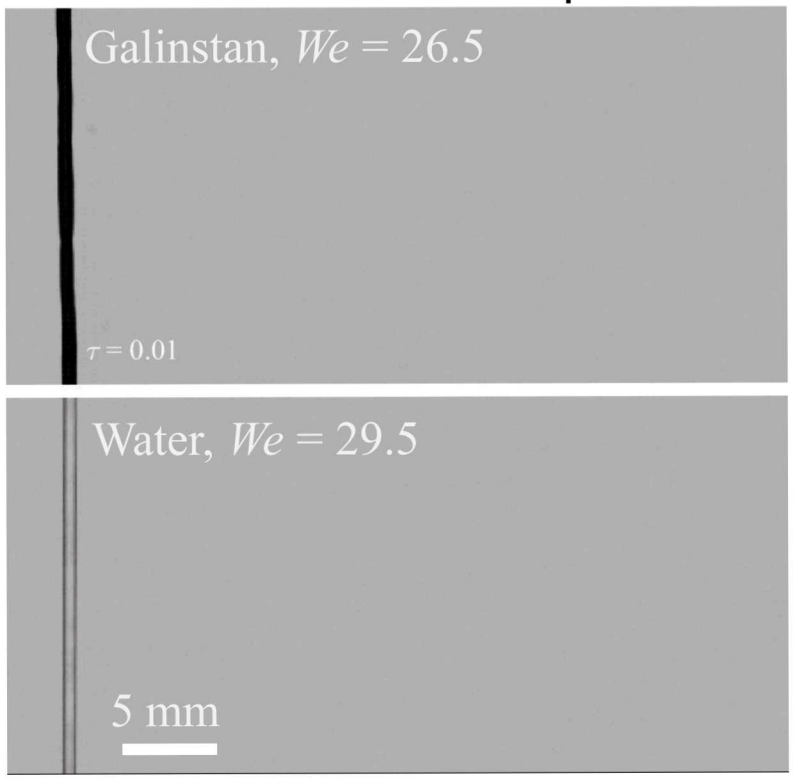

d = 0.84 mm
Galinstan Conditions: Ma = 1.24, u = 127.8 m/s, ρ_g = 1.39 kg/m^3
Water Conditions: Ma = 1.09, u = 47.9 m/s, ρ_g = 1.12 kg/m^3

Sheet-Thinning Breakup

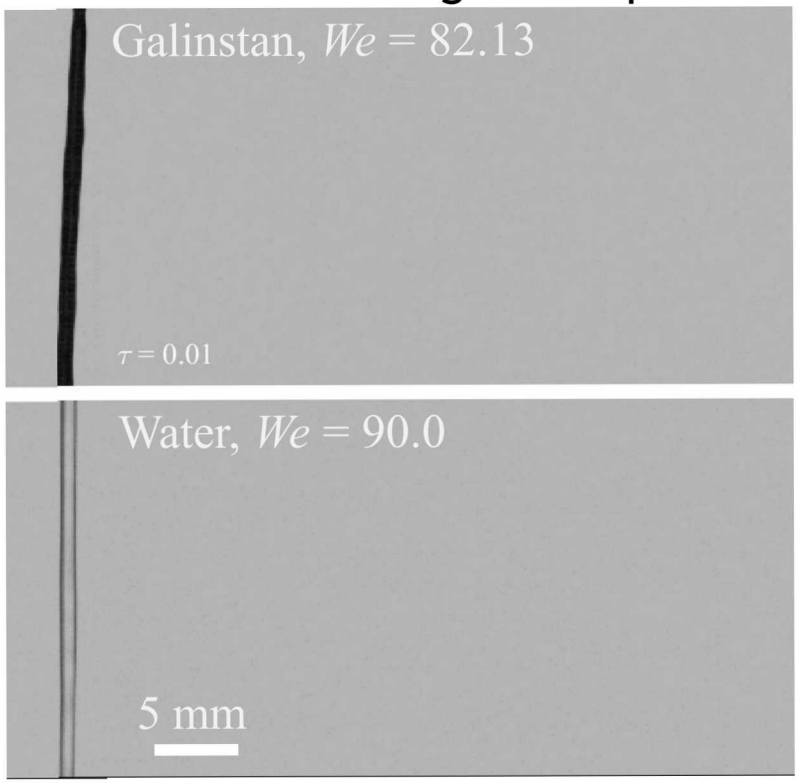

d = 0.84 mm
Galinstan Conditions: Ma = 1.12, u = 66.3 m/s, ρ_g = 1.18 kg/m^3
Water Conditions: Ma = 1.04, u = 23.5 m/s, ρ_g = 1.04 kg/m^3

- Galinstan bags break earlier and are smaller (lower deformation ratio and thicker bag walls than water)
- Galinstan bag breakup tends to have sharp edges and droplets are non-spherical, (this may be due to the oxide skin)
- Secondary droplets of Galinstan travel faster due to the higher convective velocity but can be non-dimensionalized

Breakup Morphology and Breakup Time

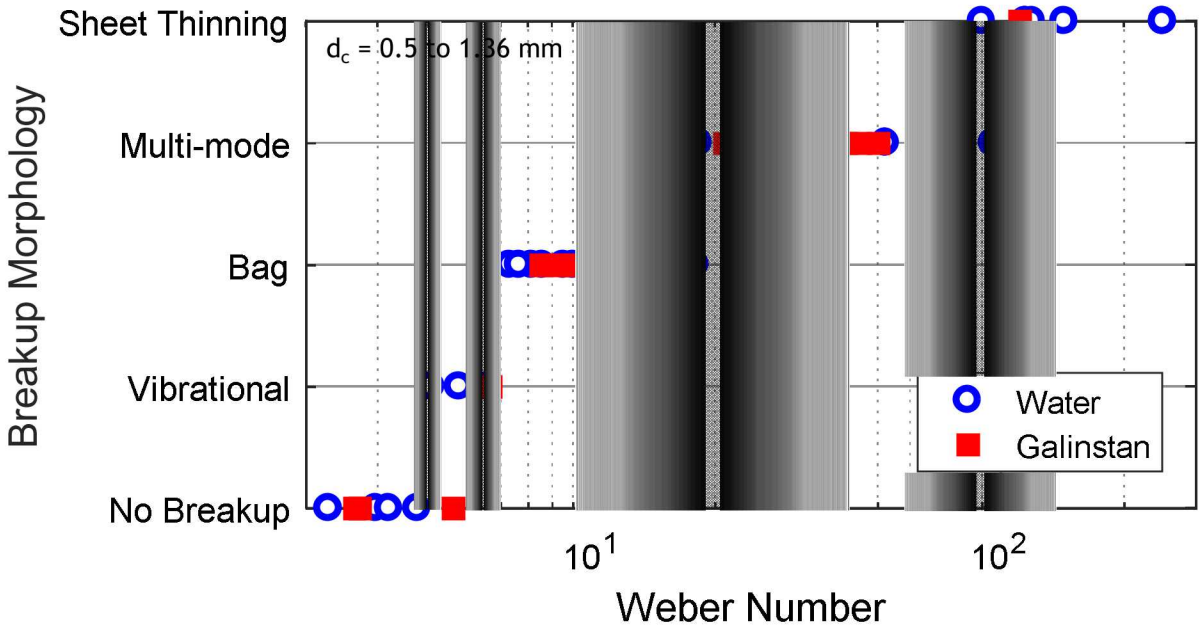

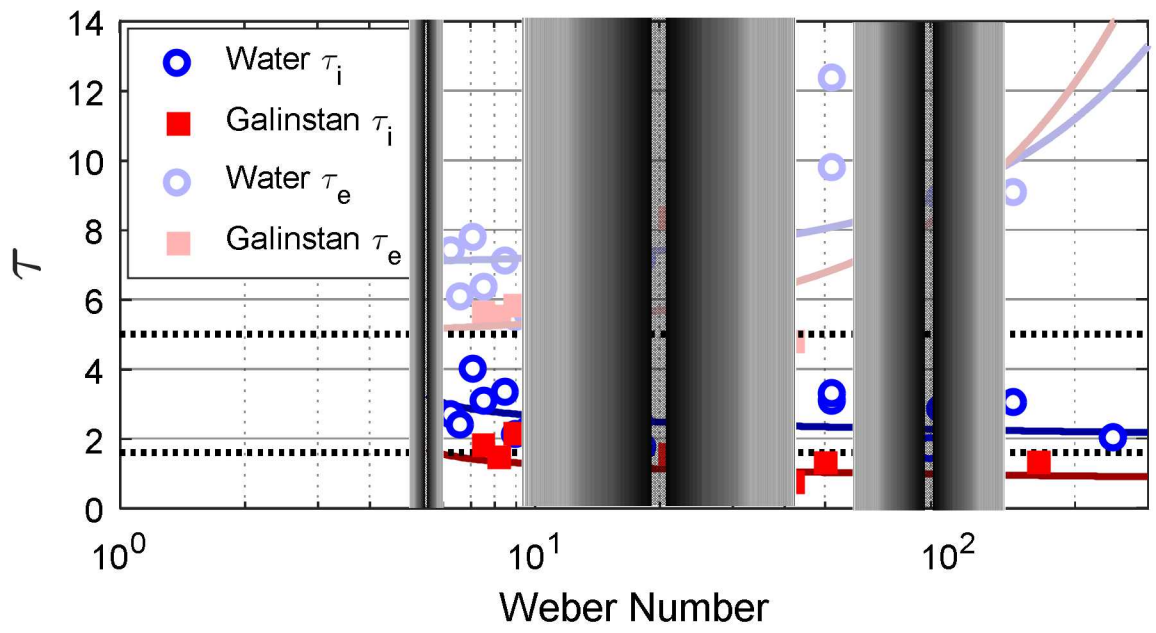

- Classifying breakup morphology is subject to uncertainties, multiple modes can occur along the column
- Galinstan experiments line up well with water experiments in terms of breakup mode
- Galinstan tends to initiate breakup earlier than water, breakup end also appears to occur slightly earlier
- In order to get statistics for non-spherical droplets, higher magnifications with depth-of-field is needed

Experimental Setup

SNL Multiphase Shock-Tube

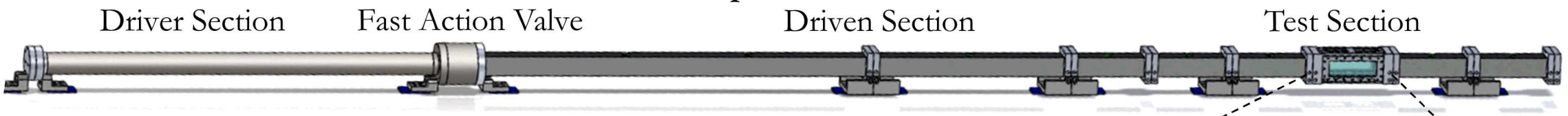

- Time-dependent, non-spherical particle sizing is difficult to conduct with conventional techniques
- DIH compares interference of diffracted and un-diffracted light[1,2], providing accurate, quantitative projected size and 3D position information
- Used Coherent Verdi 532 nm laser, spatially filtered and expanded to fill the FOV
- Made measurements as a function of downstream position x_c
- 2× camera (640 ×280 pixels at 100 kHz) was used to help track droplets
- 6× (1024 ×1024 pixels at 20 kHz) camera was used to determine extend particle size dynamic range

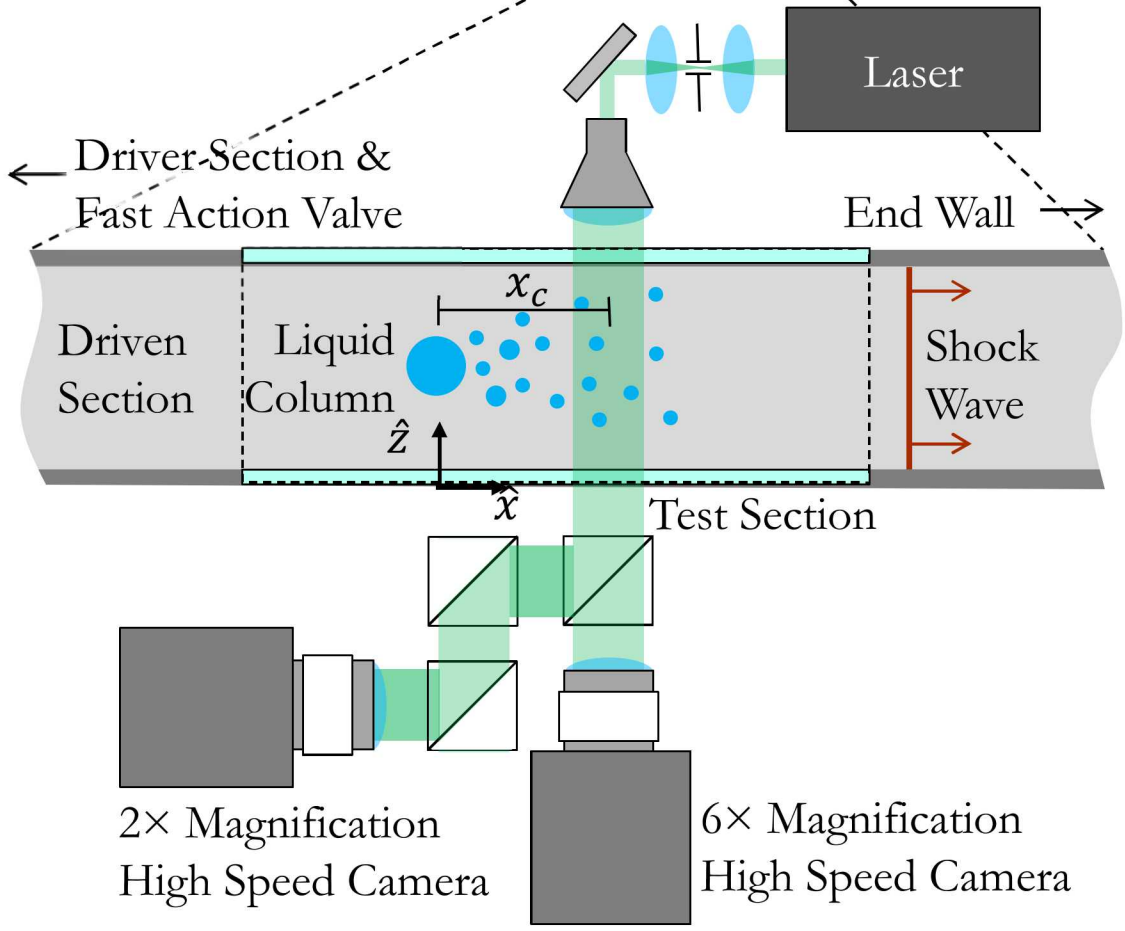

Top View - Digital In-line Holography

[1] D. Gabor, 1948
[2] U. Schnars and W. Juptner, 1994

Digital In-line Holography

- DIH is ideal for imaging and quantifying particles that may be out-of-focus at high magnifications
- Collimated light propagates as described by the diffraction equation

$$E(x,y;z) = [h(x,y)E_r^*(x,y)] \otimes g(x,y;z)$$

h – hologram, E_r^* is the planar reference wave, g – diffraction kernel, Different z-slices examined using amplitude $A = |E(x,y;z)|$

- In DIH, particle z-locations and diameters identified with minimum amplitude maximum Tenengrad method
- Tracking conducted across multiple frames using nearest neighbor and particle size cost function
- Processing was conducted on the SNL ODIN high capacity GPU accelerated CPU cluster

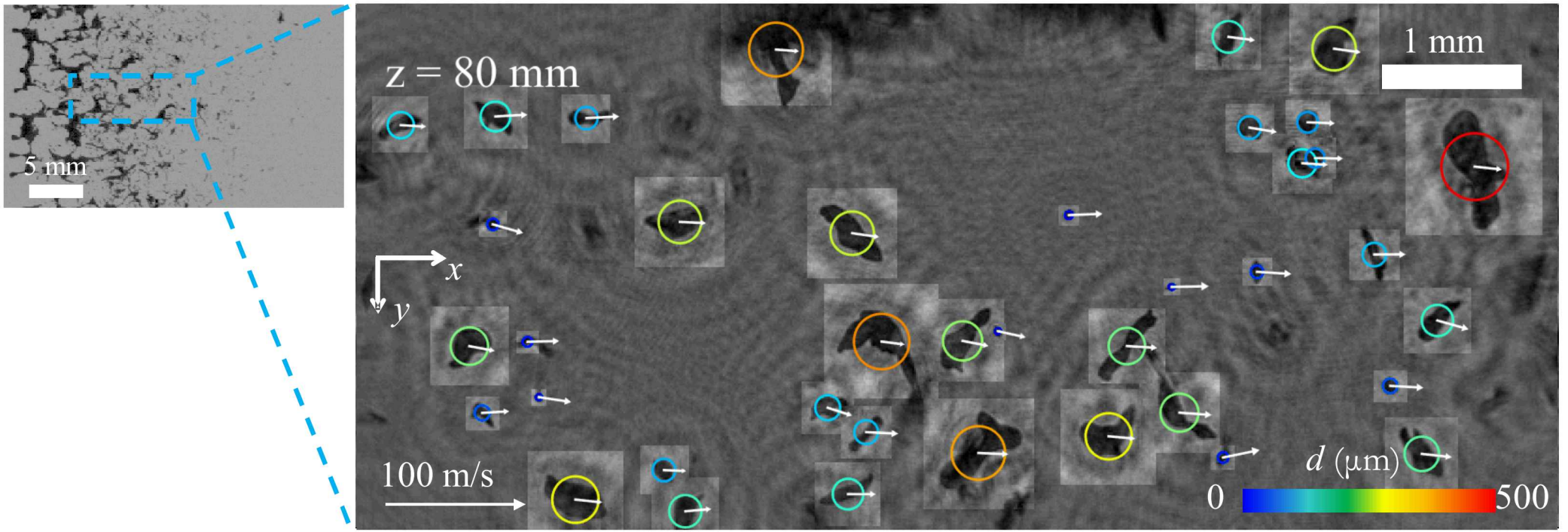

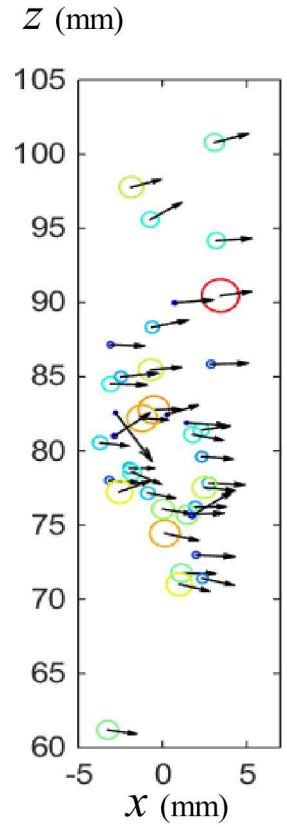

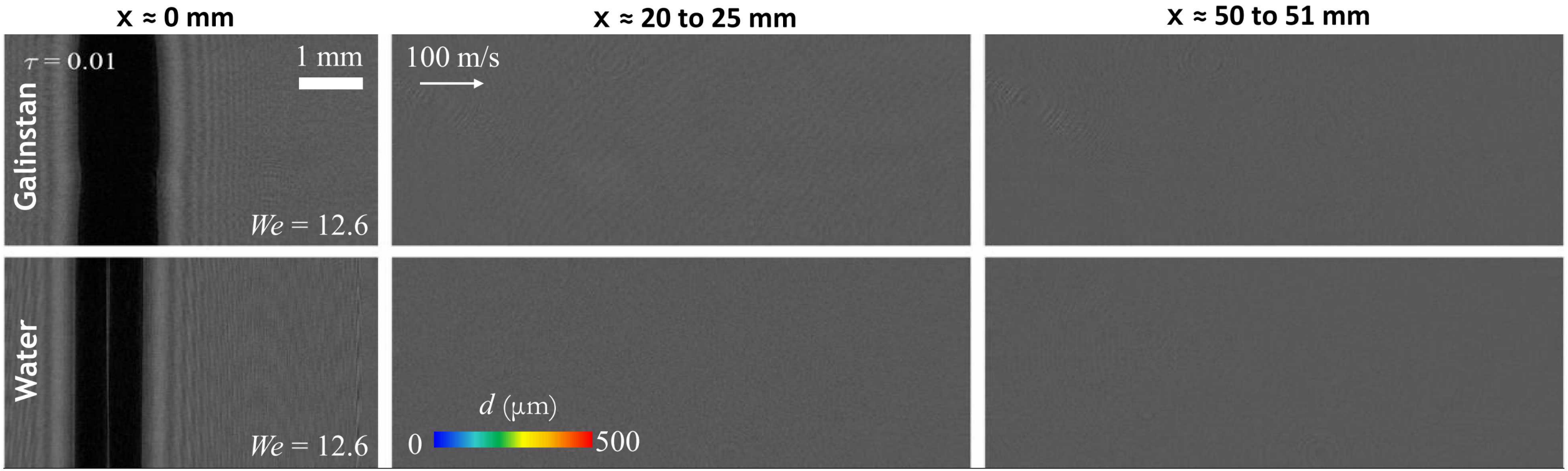

- Three tests conducted at each position for each fluid, tracked 1200 to 5700 particles for each condition
- Breakup morphologies are similar
- Galinstan breaks up earlier in non-dimensional time
- Galinstan droplet shapes are jagged due to fast surface oxide formation
- Smaller particles are generated from bag breakup and larger particles are generated from column breakup

Detailed Column Motion

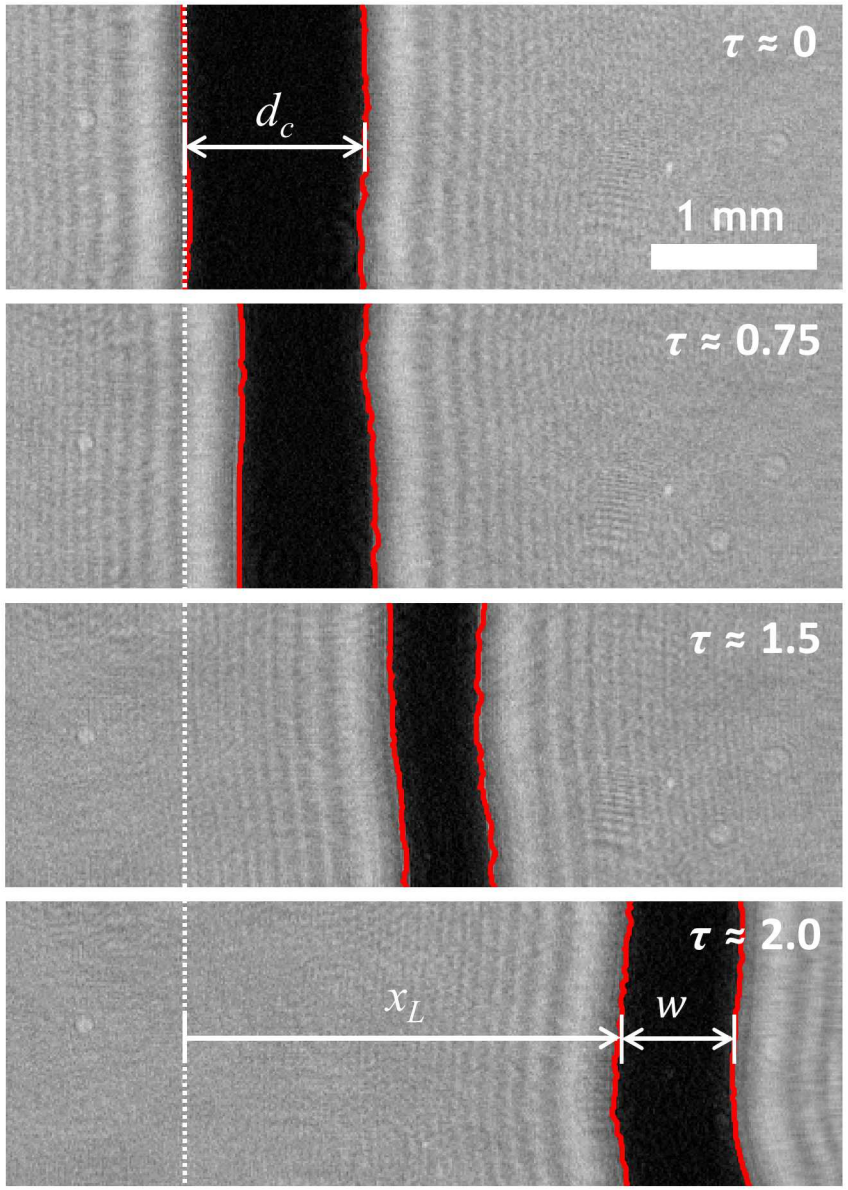

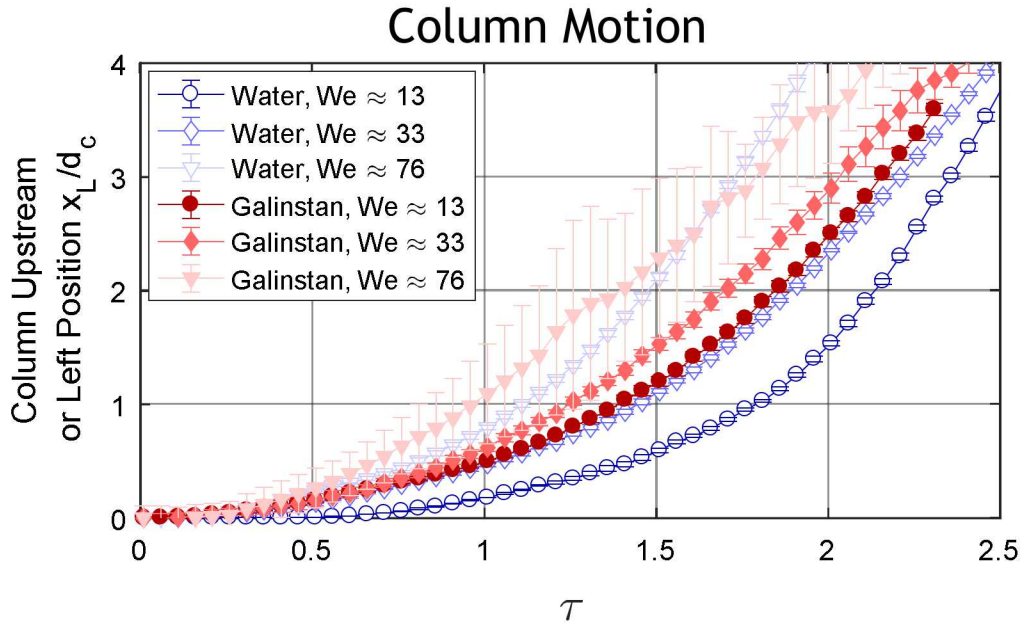

Both fluids appear to have similar column motion

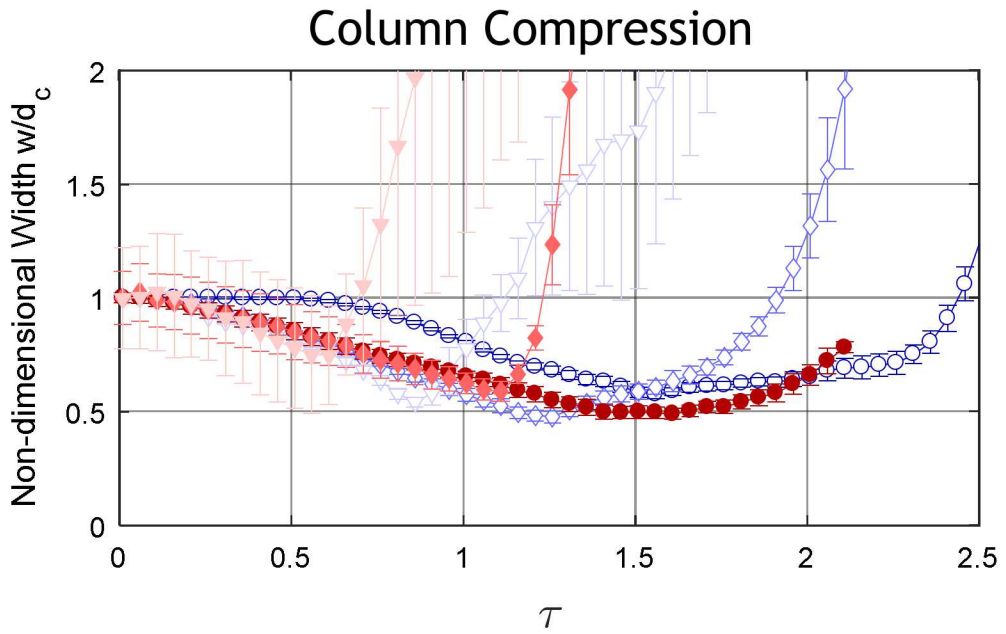

Galinstan shows earlier column breakup even in higher resolution DIH results

Column Drag

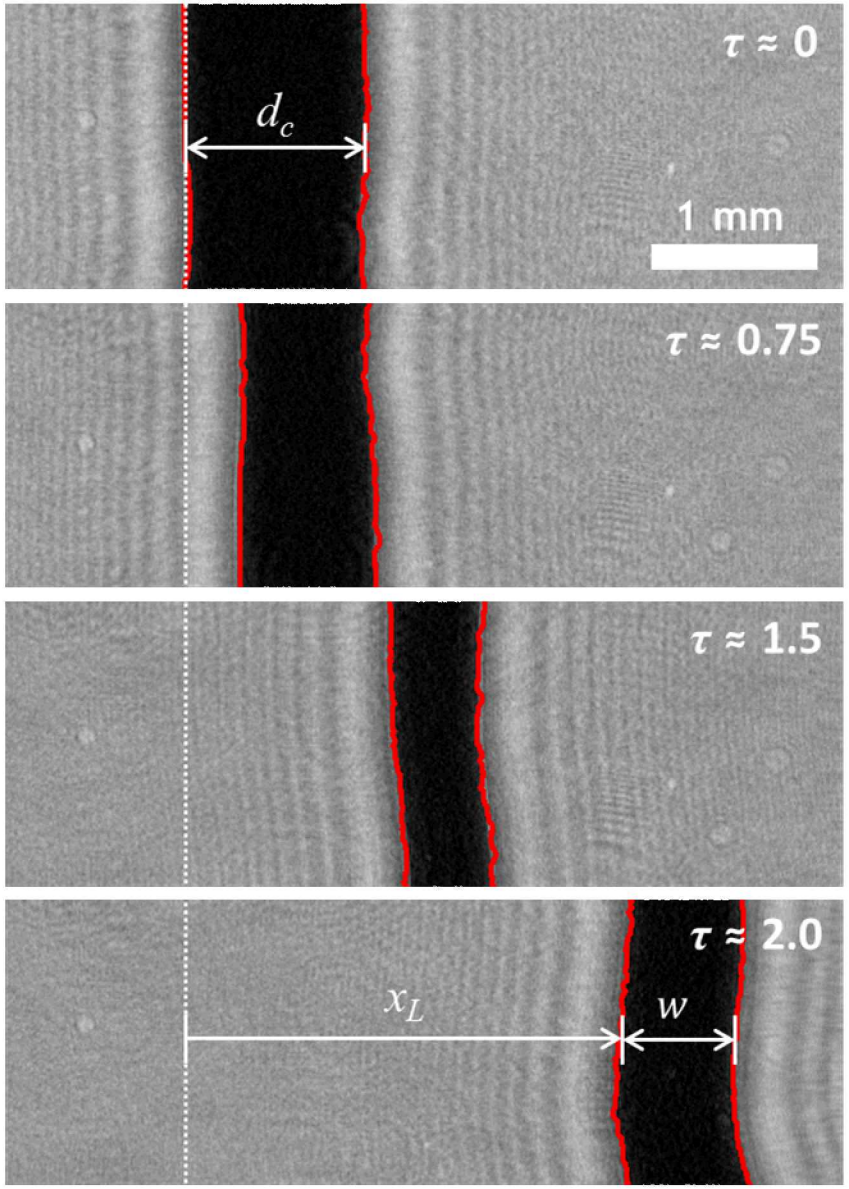

Assume constant acceleration due to drag

$$\frac{d\Delta u}{dt} = -\frac{1}{2} C_d \rho_g \Delta u^2 \frac{A}{M}$$

$$A/M = 4/(\pi \rho_l d_c) \qquad \Delta u = u_g - u_{cx}$$

Integrate using initial condition $\Delta u = u_g$ at $t = 0$

$$C_d(\tau) \approx \frac{\pi}{2\tau} \sqrt{\frac{\rho_l}{\rho_g}} \frac{u_{cx}(\tau)}{u_g - u_{cx}(\tau)}$$

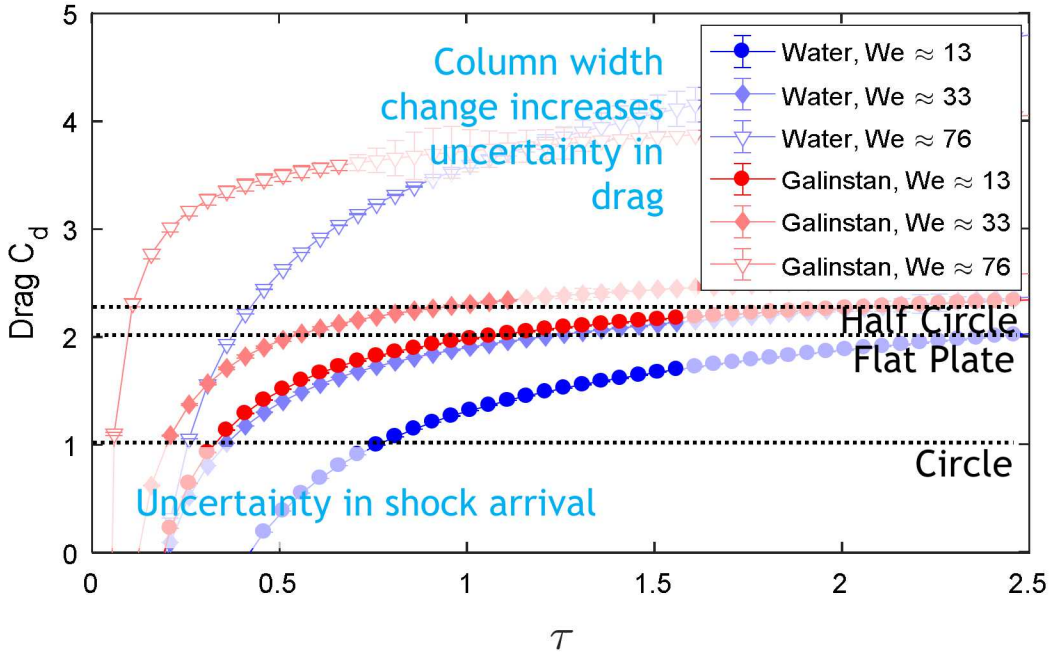

Galinstan drag is slightly higher than water due to higher gas velocity.

Approaching the sheet-thinning regime, drag increases significantly.

Droplet Velocity and Diameter

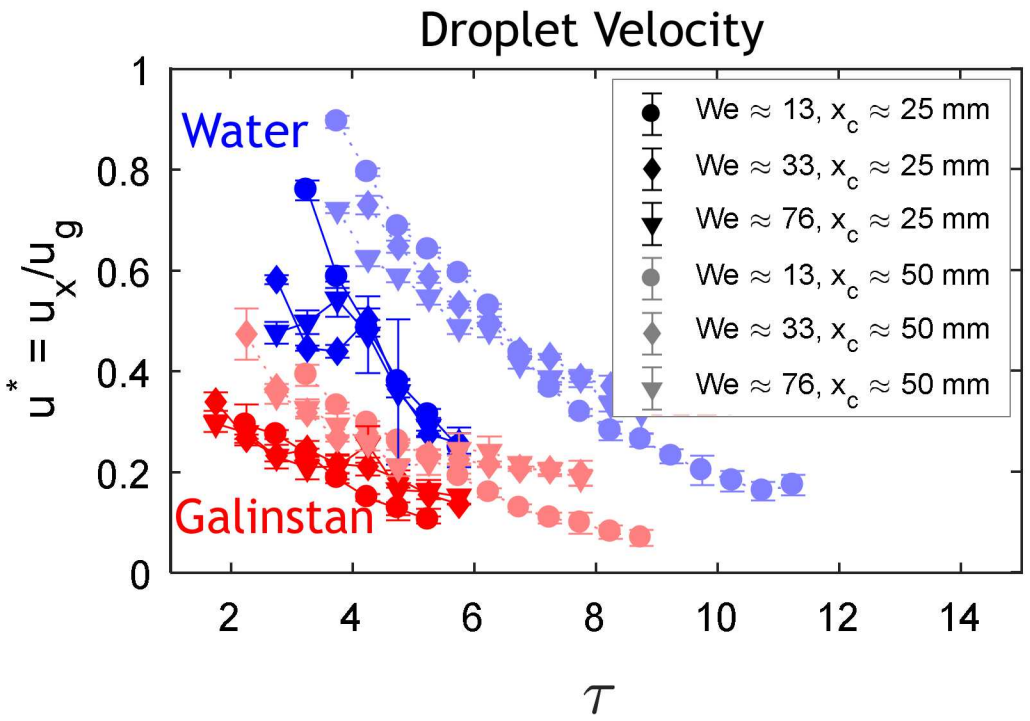

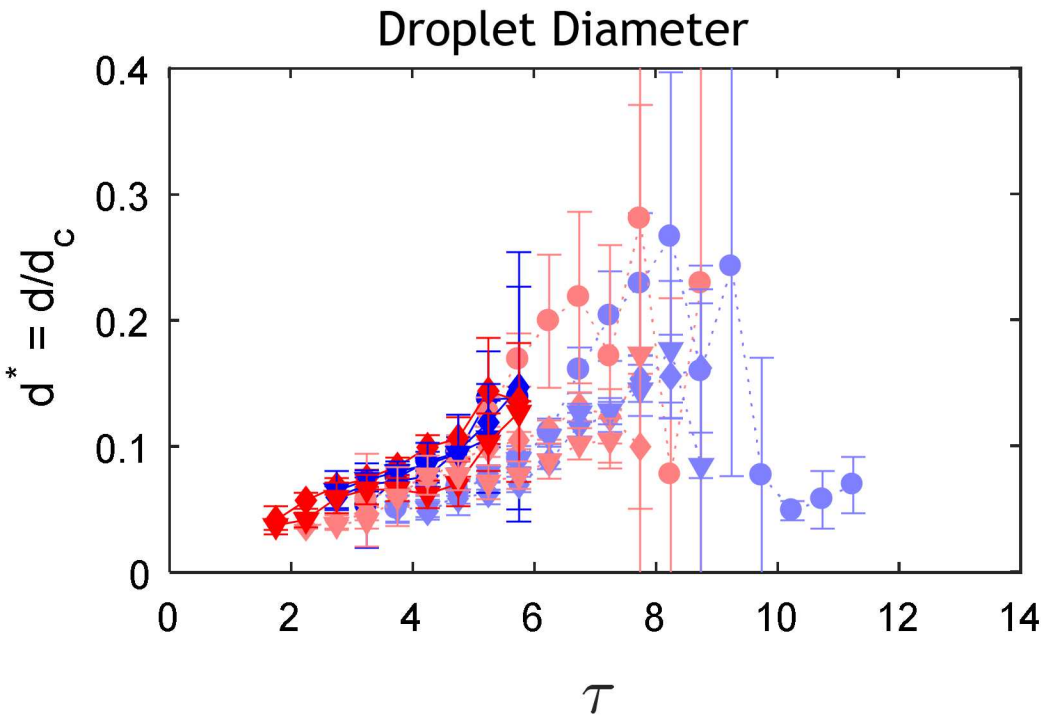

- Two downstream positions are compared (25 and 50 mm)
- Velocity non-dimensionalized with gas velocity collapses each downstream position and fluid type onto a single curve
- Droplet diameters increase with non-dimensional time
- Smaller droplets appear to be generated earlier and travel at a higher velocity

Droplet Size-Velocity Correlation

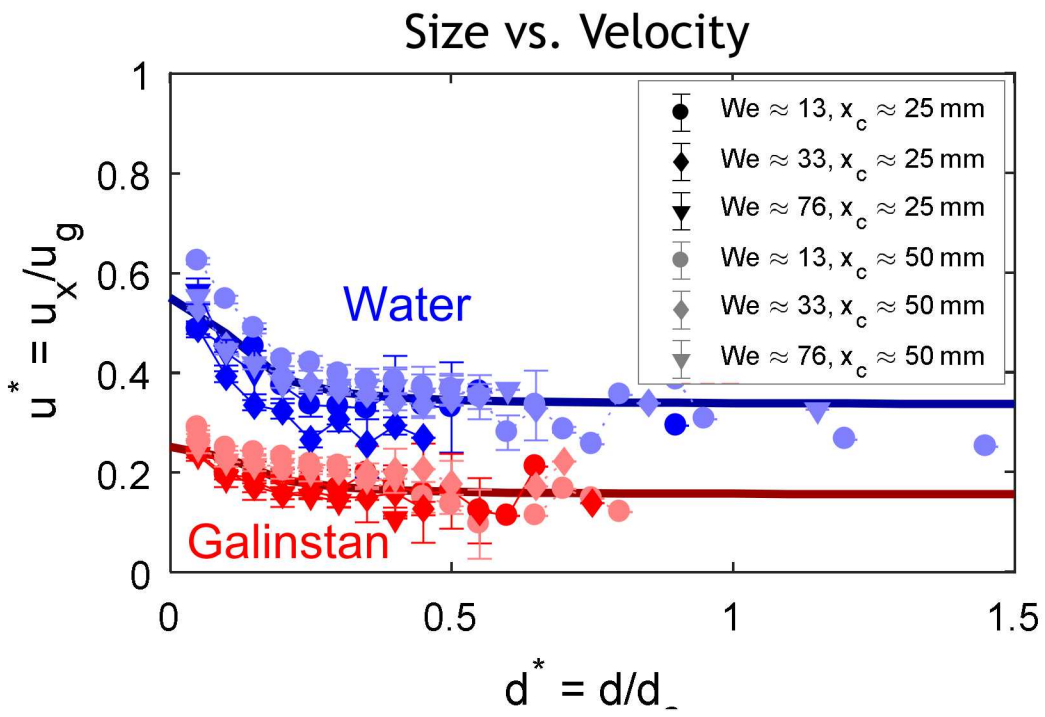

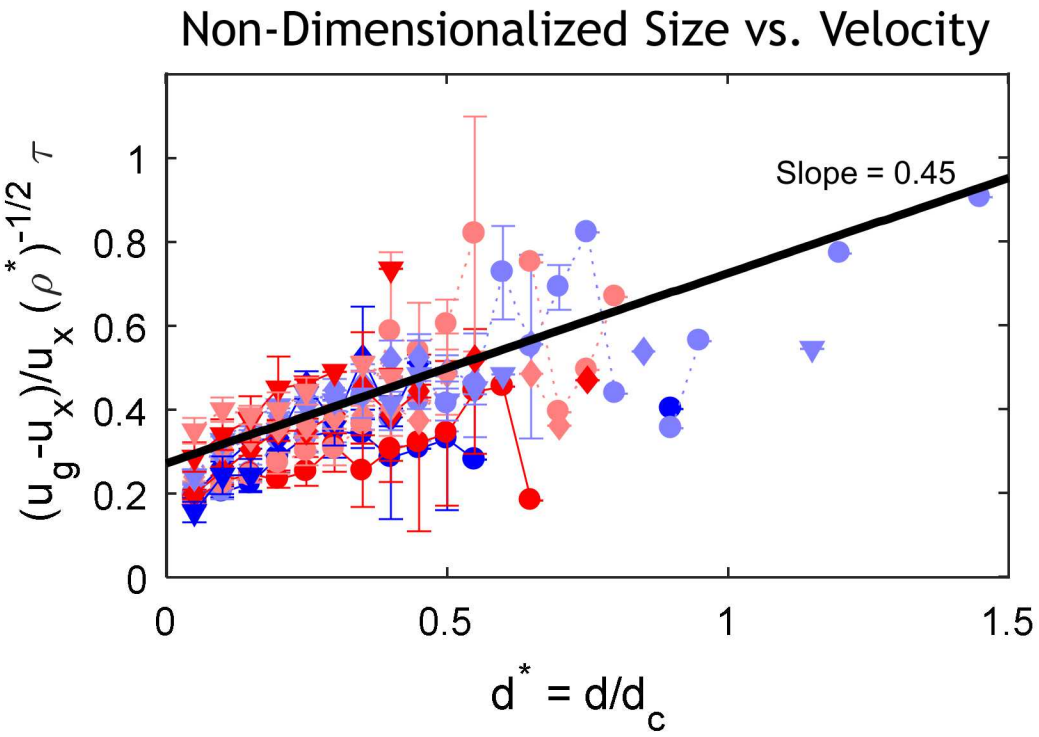

- A size-velocity correlation collapses into two curves, one for water and one for Galinstan
- By non-dimensionalizing using the density ratio, both curves collapse into a single curve
- A more detailed derivation utilizing constant acceleration due to drag (also containing the density ratio) also allows both fluids to collapse onto a single curve

$$\frac{u_g - u_x}{u_x}\sqrt{\frac{1}{\rho^*}}\tau = \frac{4}{3C_{dd}}\frac{d}{d_c}$$

Size Probability Distributions

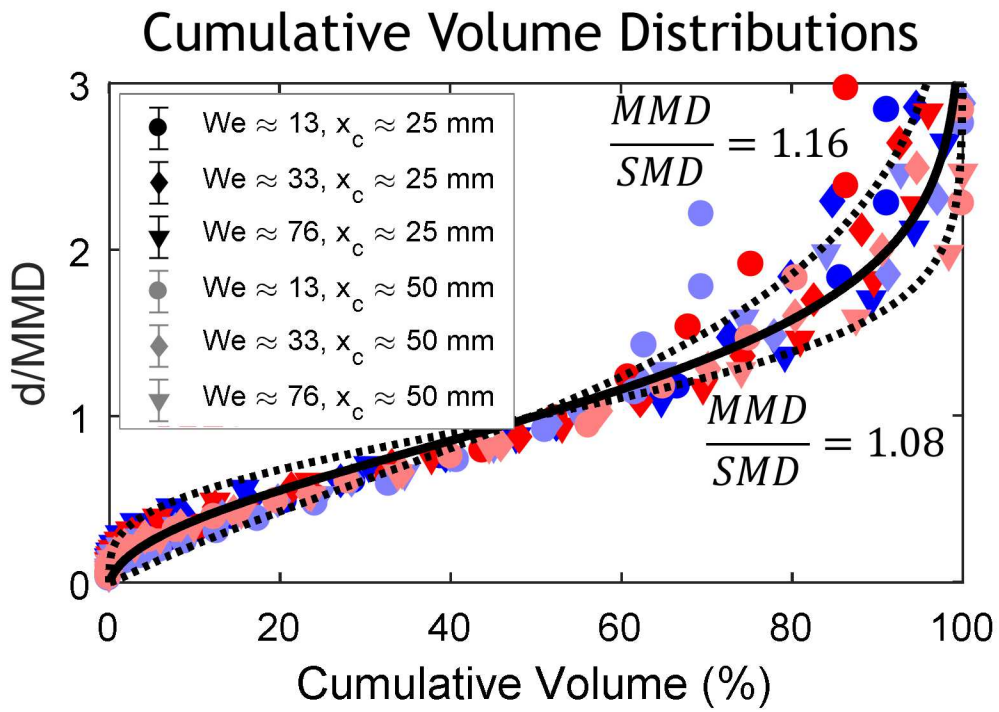

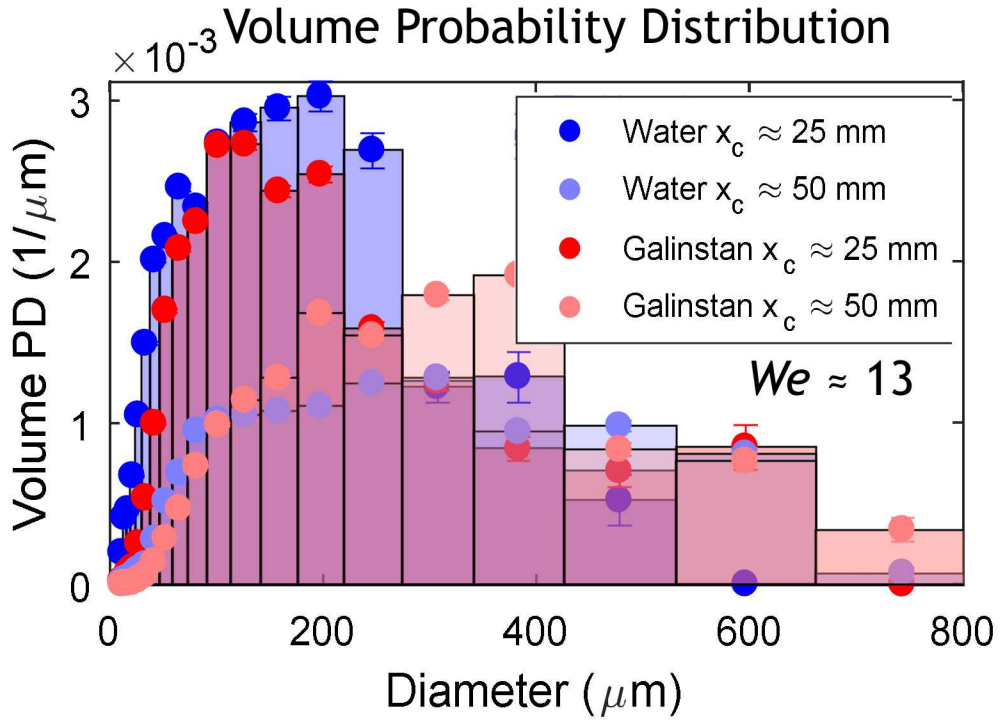

- Number probability distributions indicate water produces more smaller droplets, a secondary peak at 50 um is noticeable
- Volume probability distributions show that water and Galinstan droplets are more similar as a function of downstream position
- The cumulative volume probability distribution shows that water and Galinstan are similar for many Weber numbers
- Lines indicate the root-normal distribution, bag breakup appears to deviate the most from this distribution

Non-spherical Droplet Shape

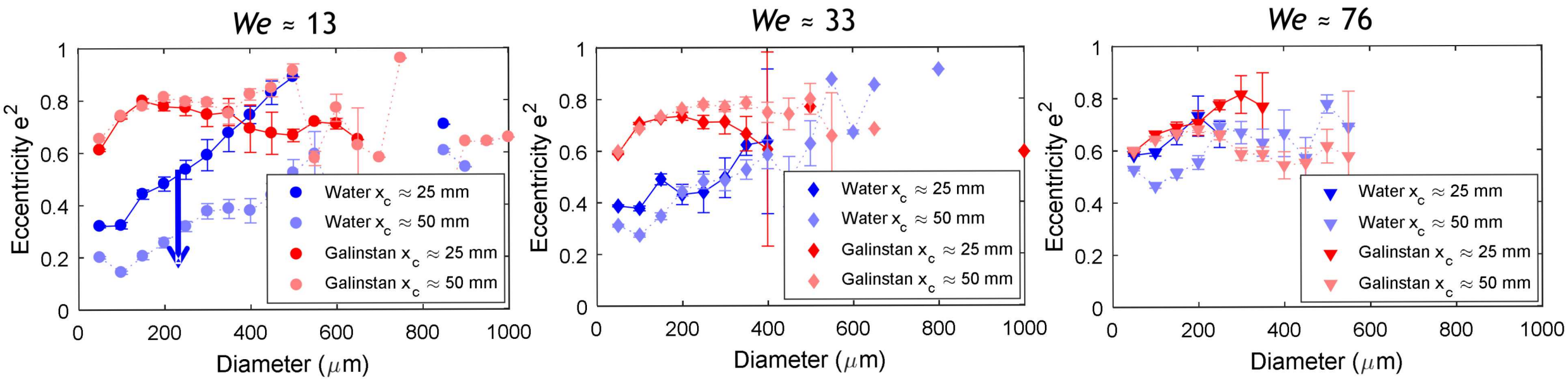

- DIH can also provide information on droplet shape
- Eccentricity $e^2 = 1\text{-}b^2/a^2$, here 0 = perfect circle and 1 = thin line
- Small water droplets are more spherical, water shape becomes more spherical further downstream
- Galinstan droplets are more non-spherical, shape is frozen and does not change further downstream
- Higher Weber numbers show more non-spherical droplets

Conclusion

- Backlit imaging provides qualitative information
- DIH provides quantitative details on column motion, 3D position, droplet size, and droplet velocity
- Galinstan has a higher density, higher surface tension, and fast passivating surface oxide formation
- Galinstan breaks up earlier in non-dimensional time
- Galinstan shows jagged breakup shapes and non-spherical droplets due to fast oxide formation
- Galinstan and water have many similar behaviors when non-dimensionalized (acceleration, droplet velocity, droplet size distributions, …)
- Additional work is needed to :
  - Understand fast-oxide formation rates
  - Obtain more streamwise DIH data (since FOV is small) so that information can be plotted as a function of non-dimensional time rather than downstream position.

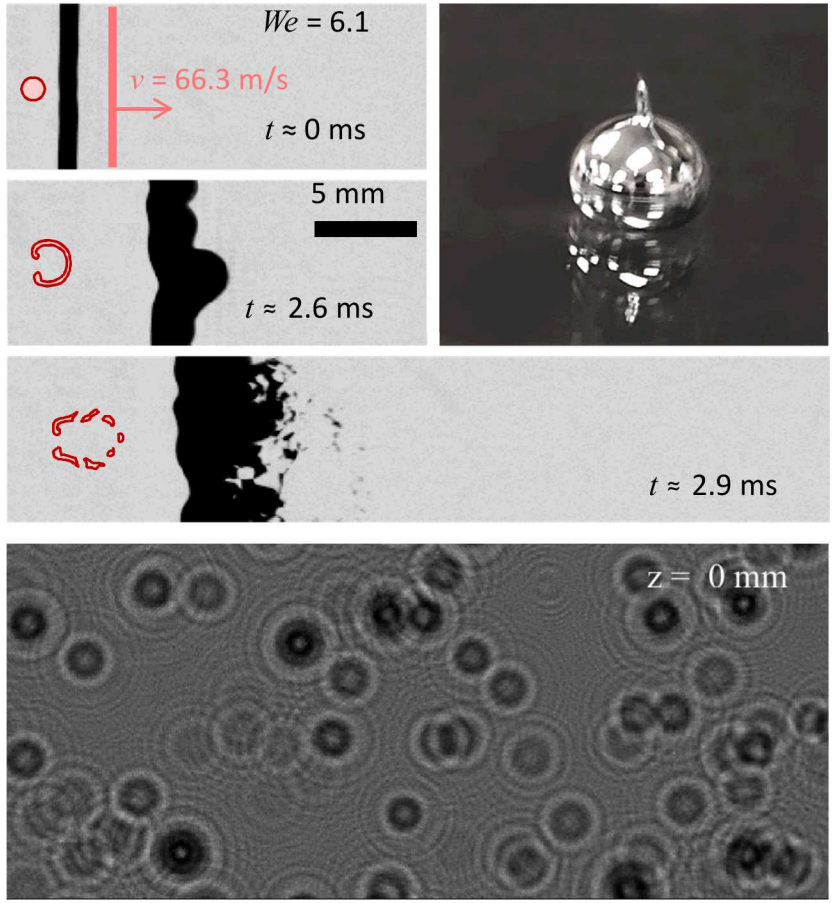

Acknowledgements

- The Laboratory Directed Research and Development program
- Marco Arienti for his work with breakup simulations.
- Edward P. DeMauro, Kyle P. Lynch, Thomas W. Grasser, Patrick D. Sanderson, Samuel W. Albert, Aaron M. Turpin, William Sealy, and Remington S. Ketchum for their help with various experiments.
- Sandia National Laboratories is a multimission laboratory managed and operated by National Technology and Engineering Solutions of Sandia, LLC., a wholly owned subsidiary of Honeywell International, Inc., for the U.S. Department of Energy's National Nuclear Security Administration under contract DE-NA0003525.

Sandia National Laboratories

U.S. DEPARTMENT OF ENERGY

National Nuclear Security Administration

Honeywell


$We = 5.5$
Questions?
4 mm
Cross-Flow

Backup Slides

Breakup Dynamics

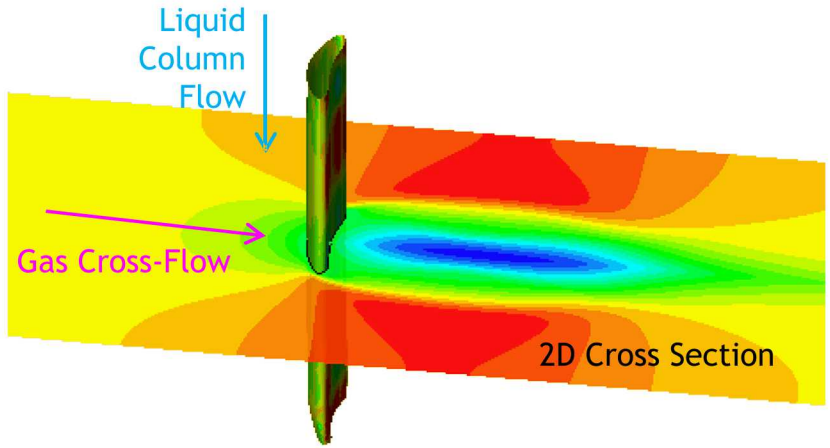

- Investigate breakup using a liquid column in a gas cross-flow (simplifies simulations and timing in experiments)
- We propose a few non-dimensional values which may contribute to different aspects of breakup
- Weber number (inertial to surface tension forces)

$$We = \frac{\rho_g u^2 d}{\sigma}$$

- Ohnesorge number (viscous to inertial forces)

$$Oh = \mu_l / \sqrt{\rho_l \sigma d}$$

- Non-dimensional time (constant acceleration due to drag) depends on the density ratio

$$\tau = \frac{tu}{d}\sqrt{\frac{\rho_g}{\rho_l}} = \frac{tu}{d}\frac{1}{\sqrt{\bar{\rho}}}$$

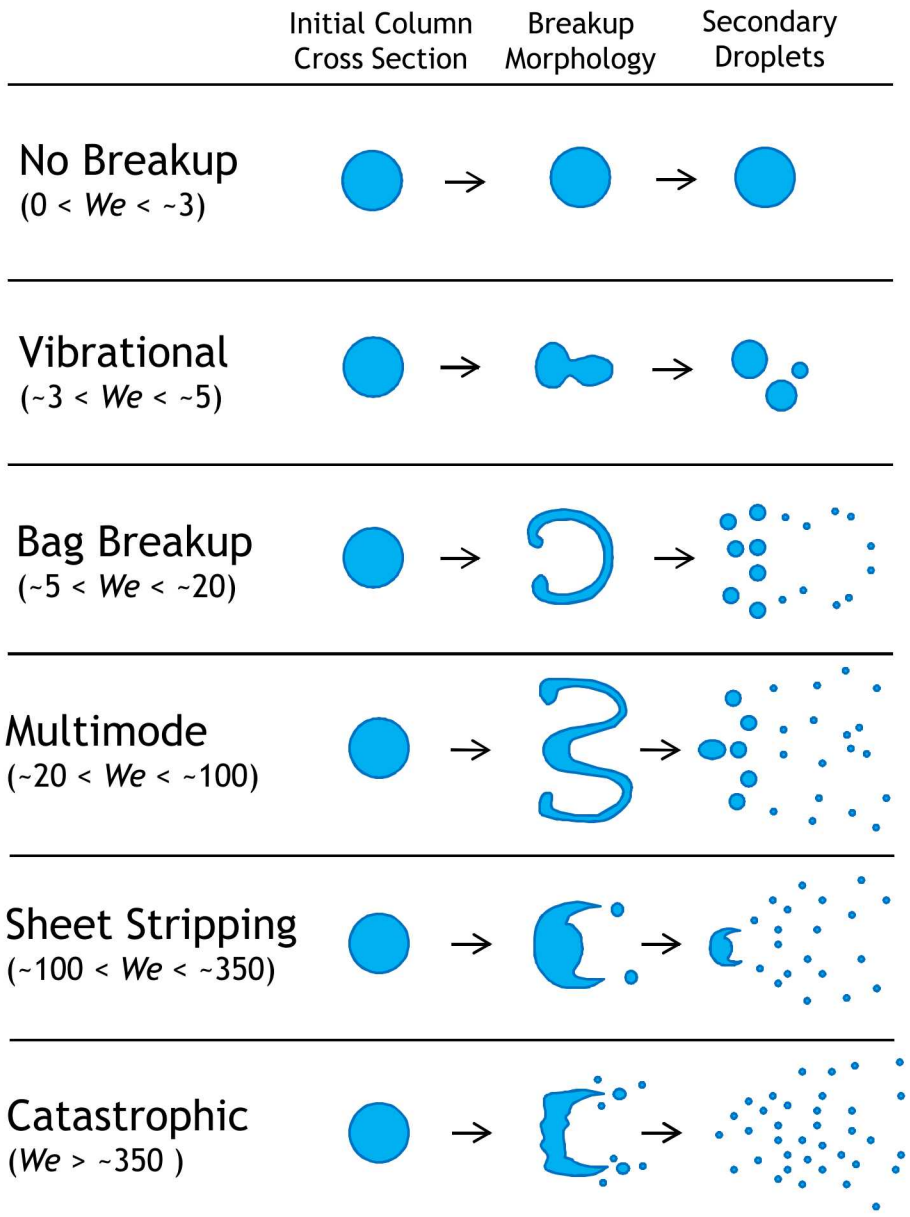

Liquid Metal Properties

- Use a non-toxic, room-temperature liquid metal to avoid heat transfer and combustion effects
- Most liquid metals form oxide layers quickly
- Galinstan eutectic alloy
  (68.5% gallium, 21.5% indium and 10% tin)
  - Melting temperature of -19 degrees Celsius
  - Alloys with aluminum and many other metals
  - Forms passivating[1], elastic oxide layers (Ga_2O_3/Ga_2O, surface yield stress of EGaIn is ~ 0.5 N/m) which prevent the formation of perfectly spherical droplets

Properties	Galinstan[2,3]	Water
Density	~ 6440 kg/m^3	1000 kg/m^3
Surface Tension	~ 0.718 N/m	0.073 N/m
Bulk Viscosity	~ 2.4 mPa·s	0.89 mPa·s

Top View of Liquid Galinstan

Side View of Galinstan Droplets

D. Kim et al. 2012

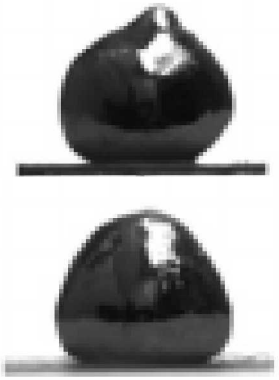

D. Kim et al. 2015

1. M. D. Dickey et al. 2008
2. C. Karcher et al. 2003, surface tension values may be influenced by the oxide layer
3. J. N. Koster 1999, viscosity not verified as a function of shear rate

2D Simulations

- Time-resolved 2D simulation developed at Sandia was used to simulate the flow[1]
  - Utilized a moment-of-fluid approach to solve for the interface
  - The surface tension is evaluated using the curvature and the ghost fluid method
  - Time step defined by the flow speed
  - Gas → perfect gas equation of state
  - Liquid → generic Tait equation of state for stiff materials
  - Utilizes adaptive mesh refinement (BoxLib) with minimum cell size of 3.9µm
  - Simulations conducted on the SNL Redsky super computer
- Oxide layer effects and fluid non-uniformities not included
- 2D simulations do not capture lengthwise perturbations in the column or some droplet formation effects which require two principal curvatures to minimize surface area.

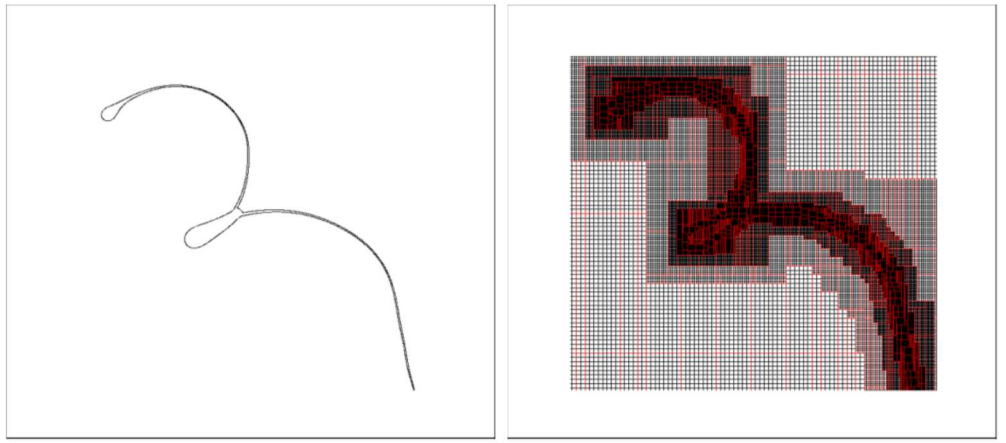

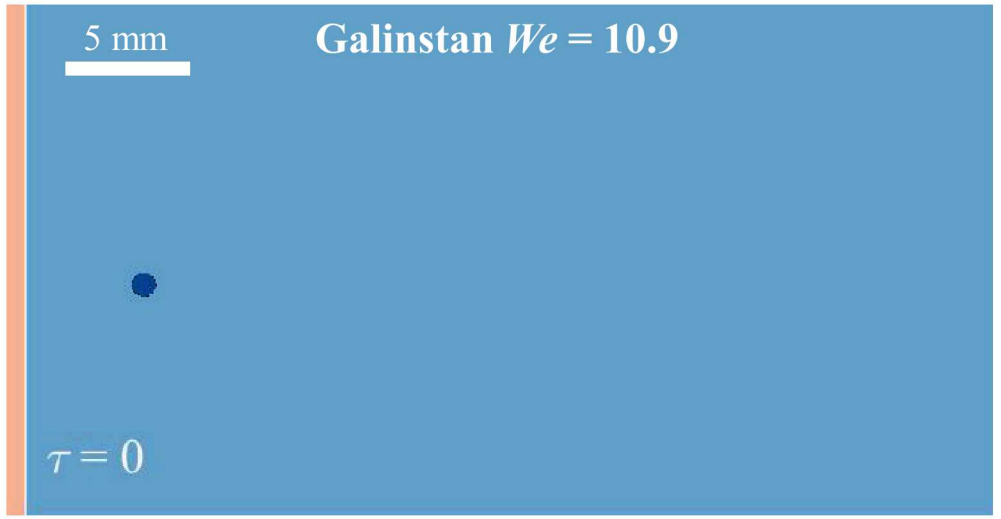

*Red/Blue background colors indicate the relative gas velocity (normalized per image) in the x-direction

1. M. Arienti et al. 2016

2D Simulation Predictions

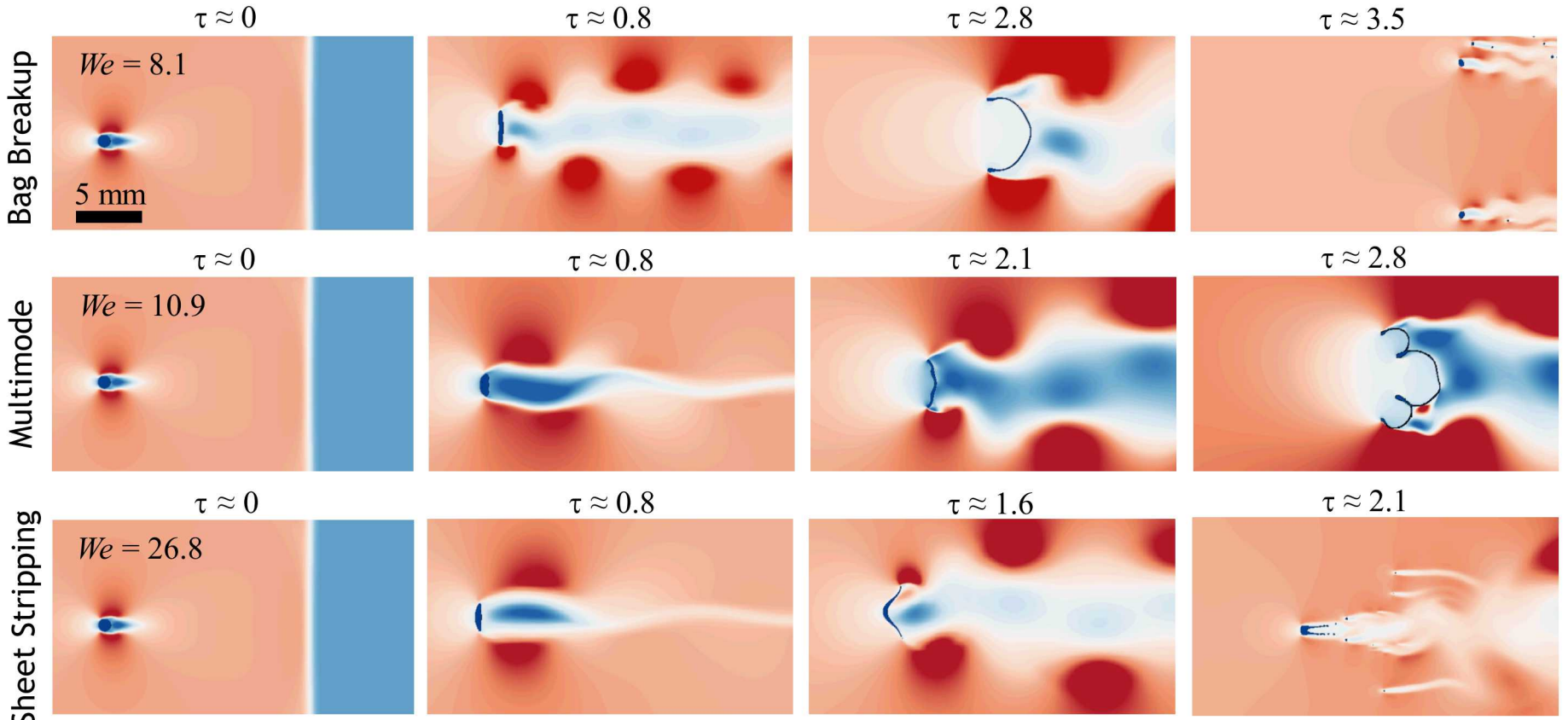

*Red/Blue background colors indicate the relative gas velocity (normalized per image) in the x-direction

- Morphology begins to appear near $\tau = 0.8$.
- Secondary droplets appear earlier as Weber number increases.
- Simulations with Galinstan properties show semi-spherical secondary droplets.

Digital In-line Holography

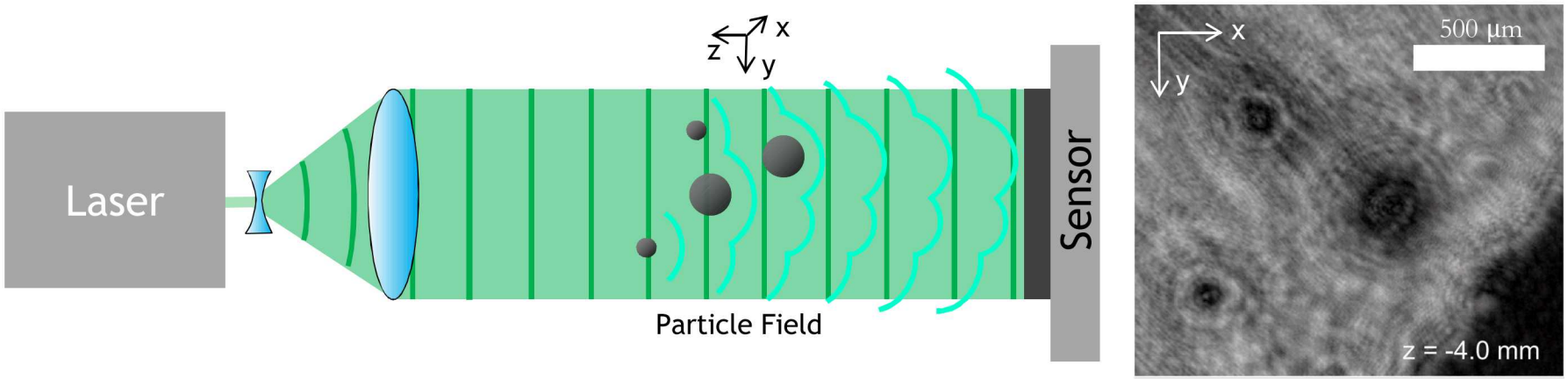

- Holography records the full field information (amplitude and phase), proposed by D. Gabor in 1948
- Digital In-line holography (DIH) compares interference of diffracted and un-diffracted light, proposed by U. Schnars and W. Juptner in 1994
- Light propagation is described by the diffraction integral equation (Rayleigh-Sommerfeld diffraction kernel)

$$E(x,y,z)=\frac{1}{\lambda}\iint E(\xi,\eta,z=0)\frac{e^{-jkr}}{r}d\xi d\eta \quad \text{where: } r=\sqrt{(\xi-x)^2+(\eta-y)^2+z^2}$$

E(x,y,0) = h(x,y)·Er* is the complex amplitude at hologram plane, h(x,y) is the hologram,
Er* is the planar reference wave, E(x,y,z) is the refocused complex amplitude at optical depth z

- Fast convolution GPU solver codes for flow diagnostics are being developed by D. Guildenbecher at Sandia

3D Breakup model and Experiment

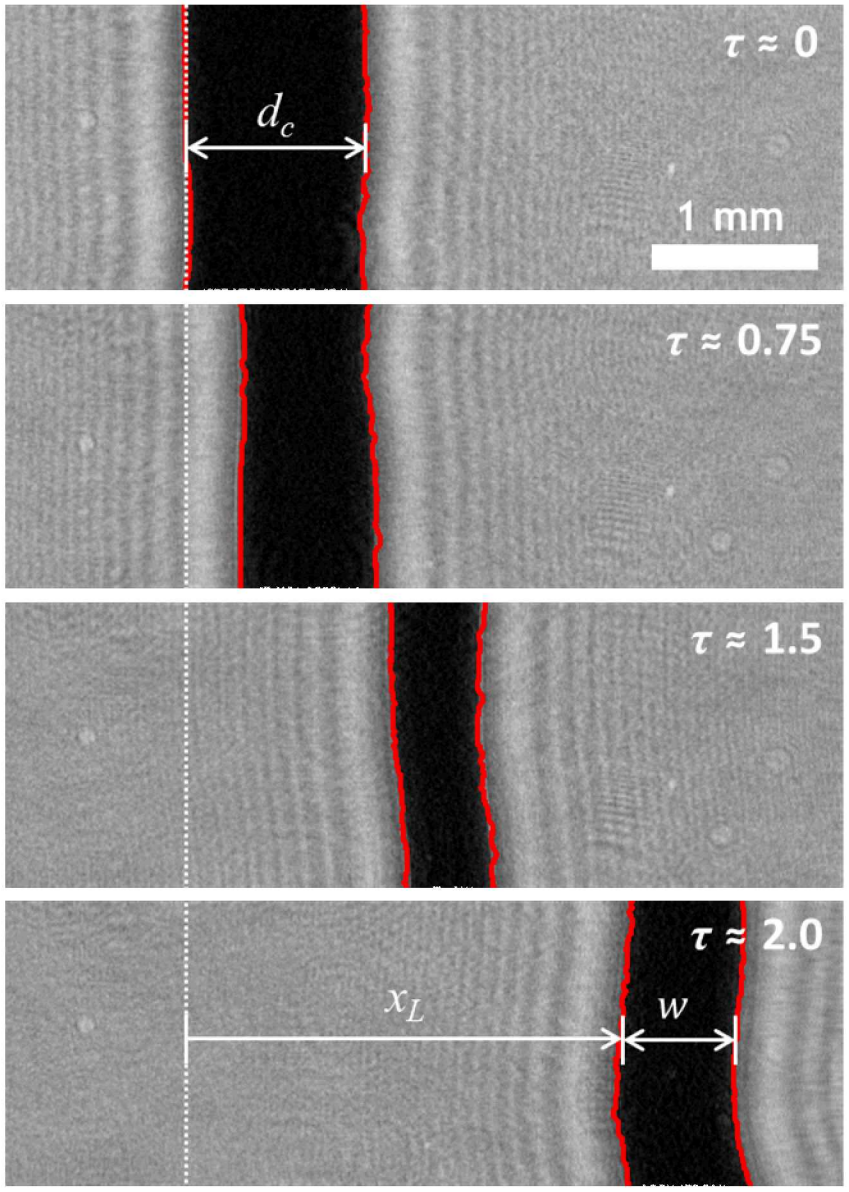

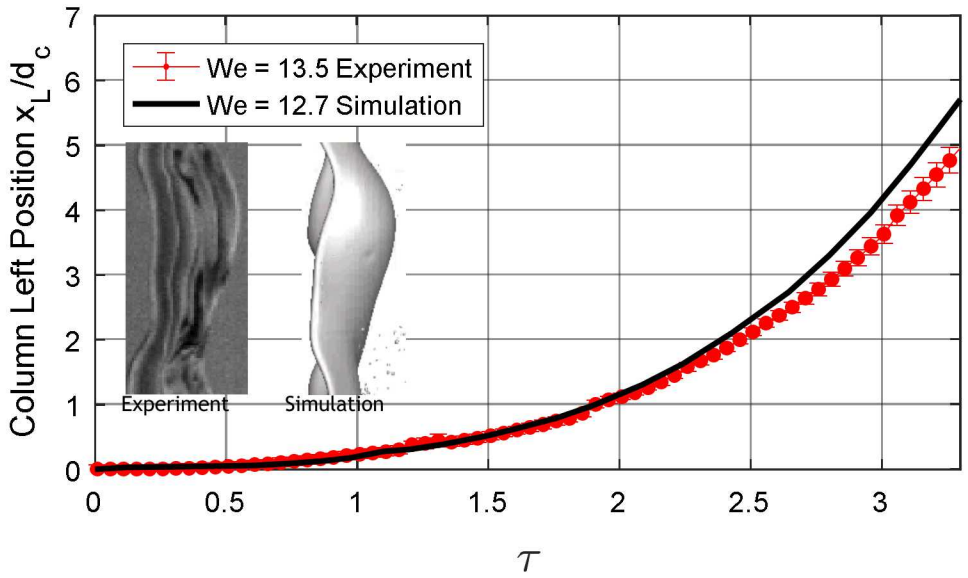

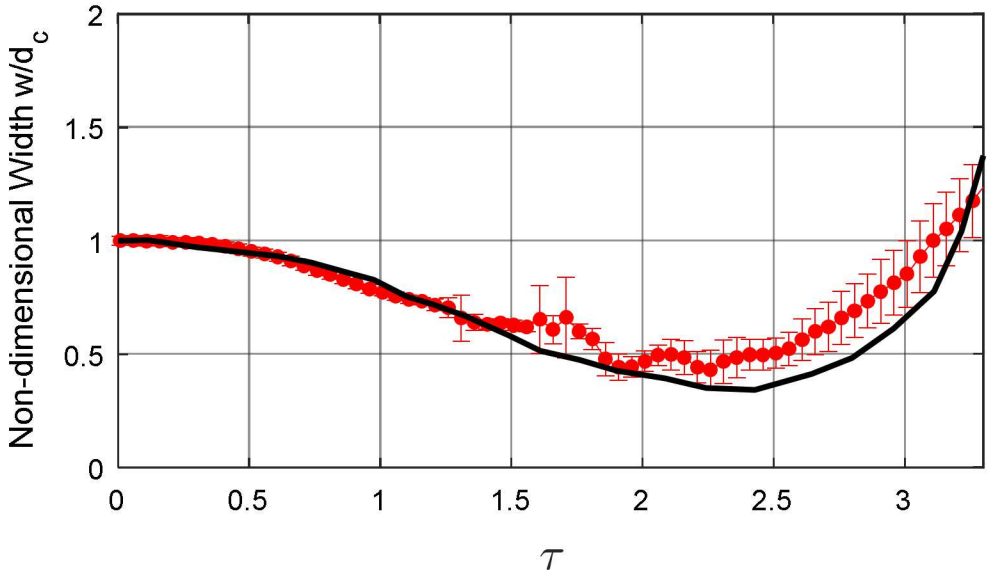

Working with Dr. Marco Arienti at Sandia California to compare validate modeling strategies

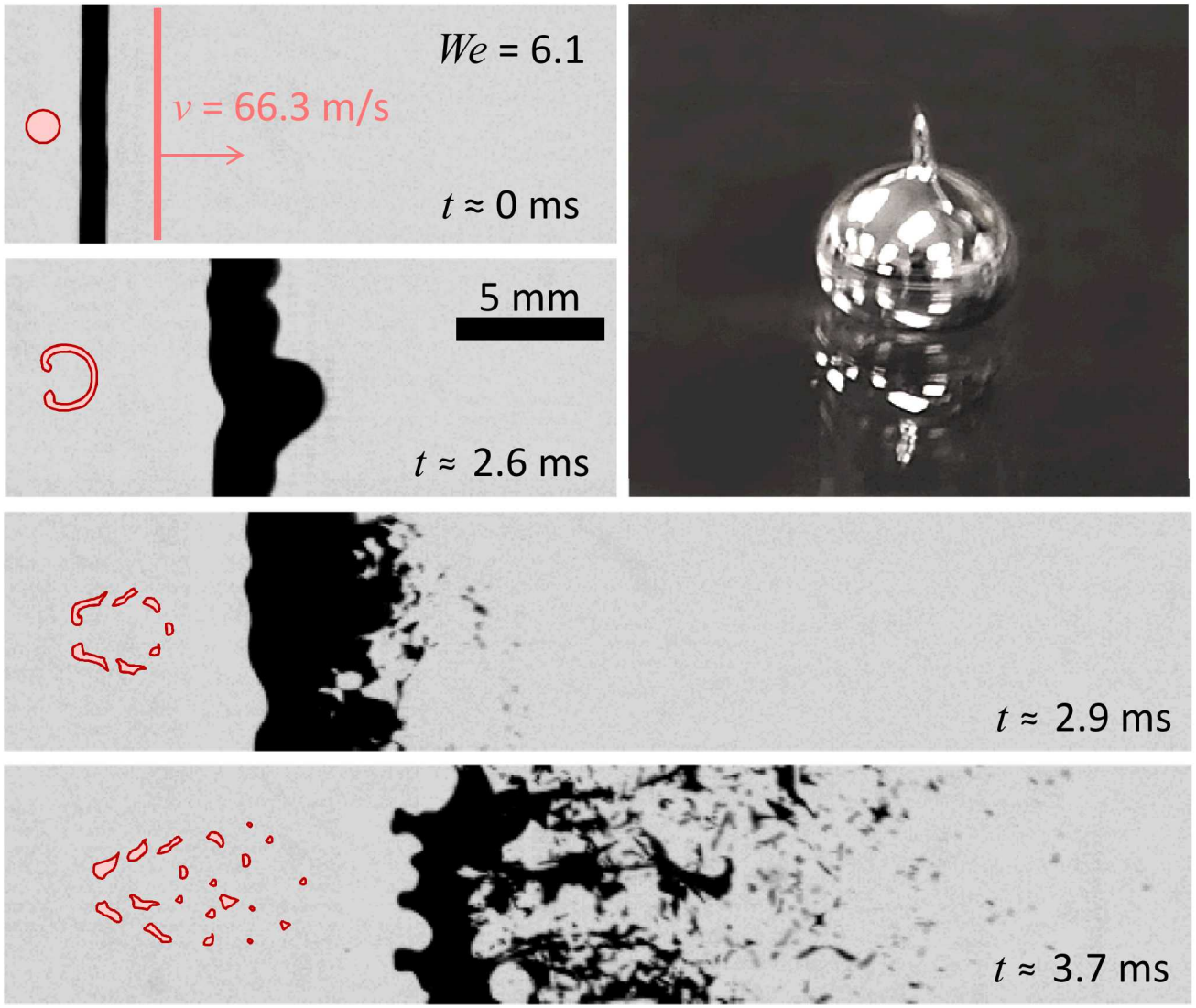
We = 6.1
v = 66.3 m/s
t ≈ 0 ms
5 mm
t ≈ 2.6 ms
t ≈ 2.9 ms
t ≈ 3.7 ms

Experimental Setup

Shock Tube Top View - Digital In-line Holography

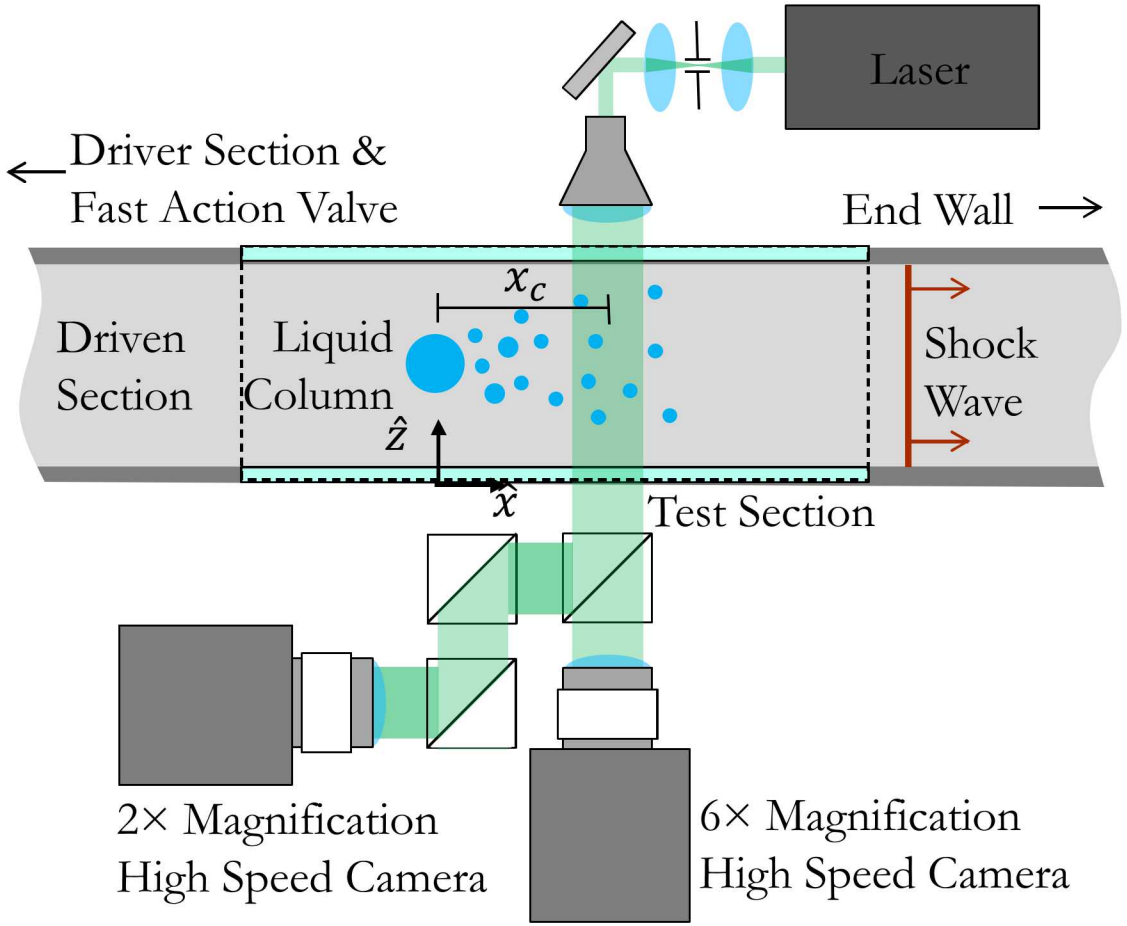

Shock Tube Side View - Fluid Delivery System

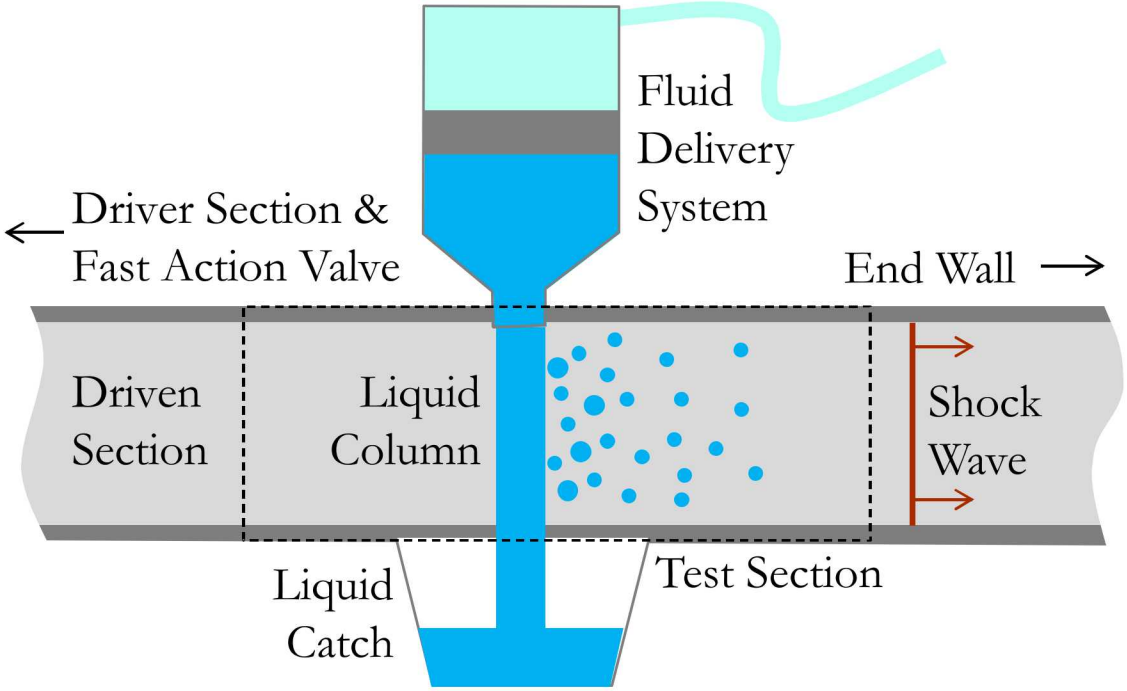

Experimental Setup

Back-lit Imaging

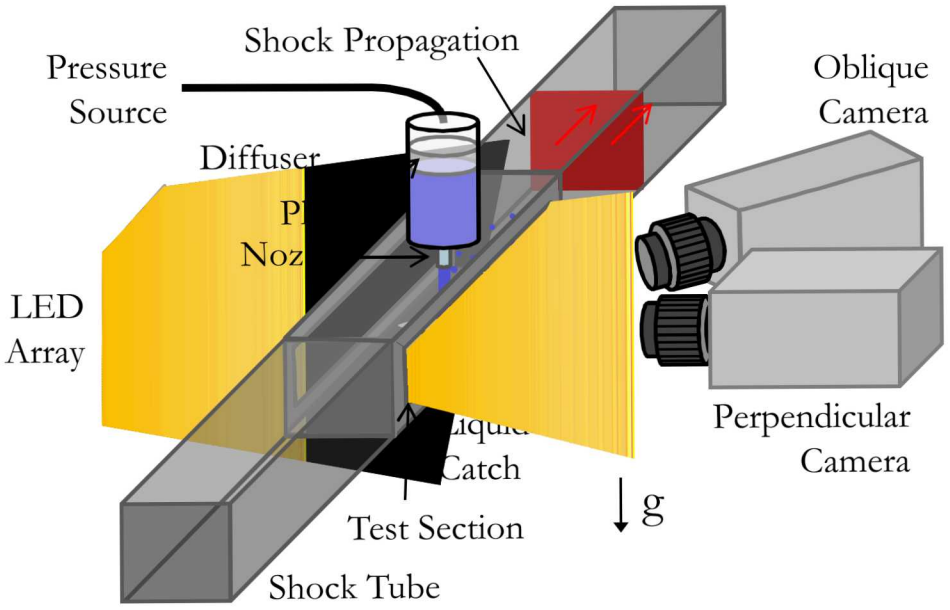

Digital In-line Holography

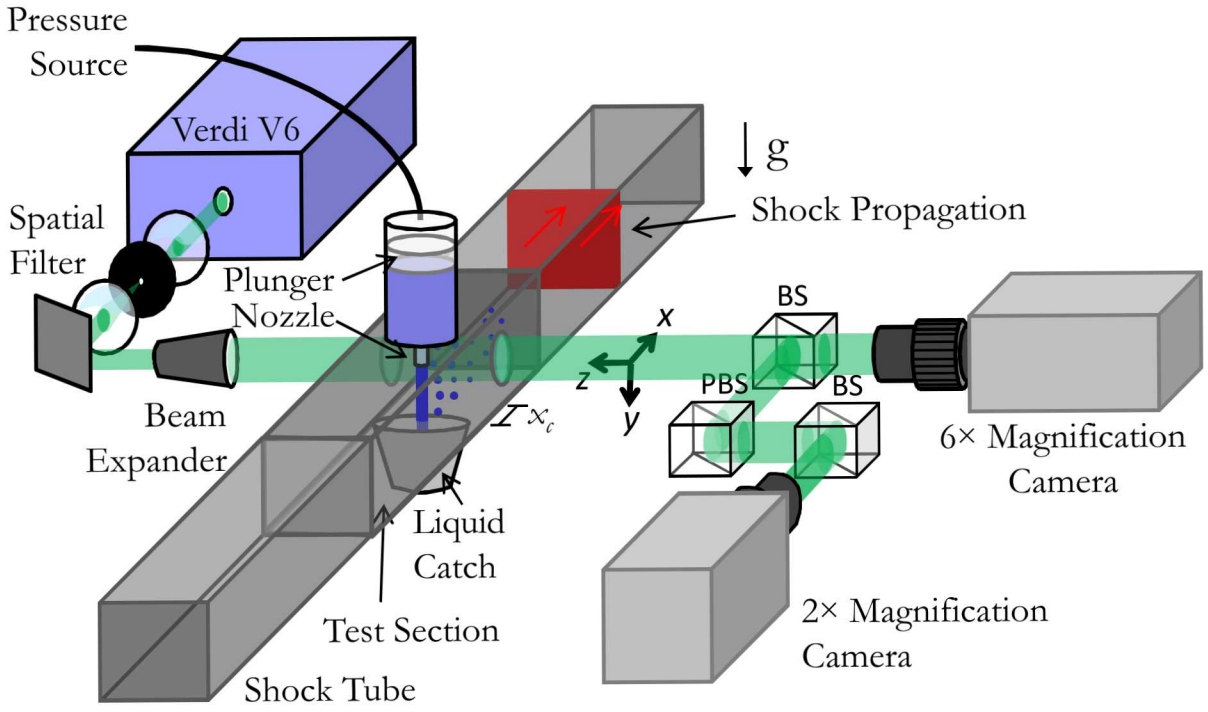

Backlit Breakup Morphology

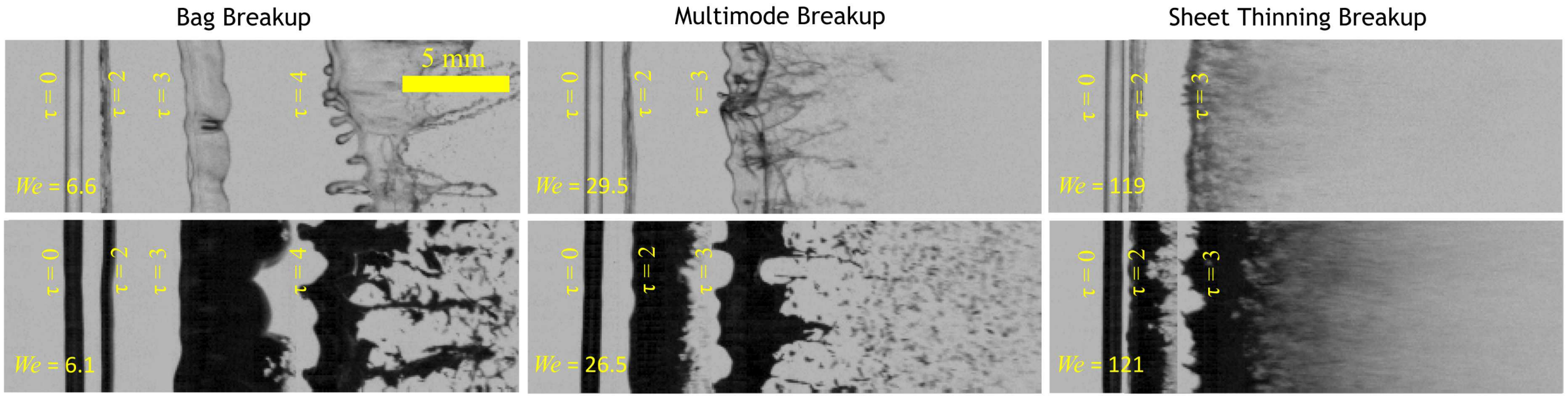

Breakup Morphologies

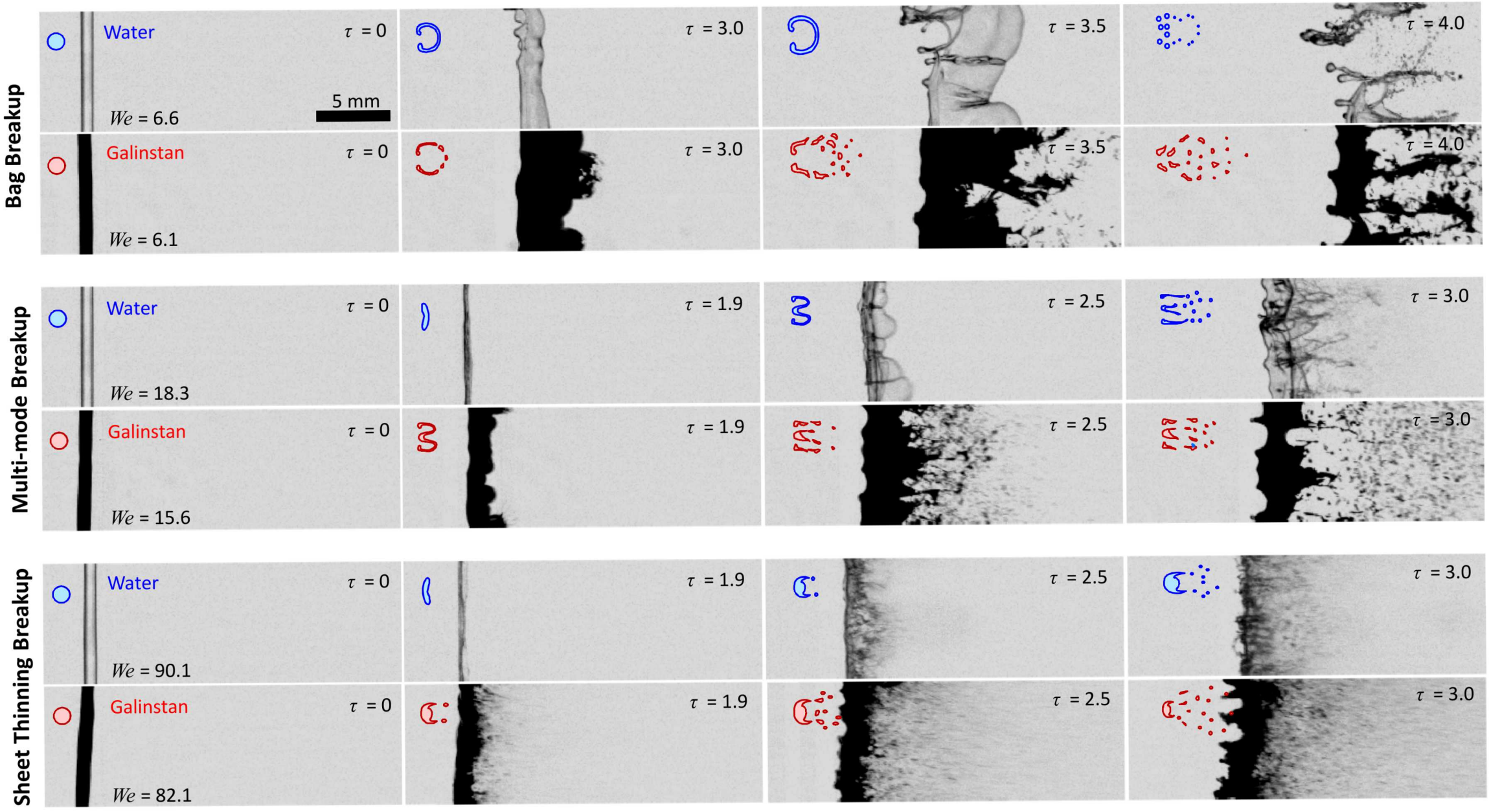

2× and 6× Fields of View

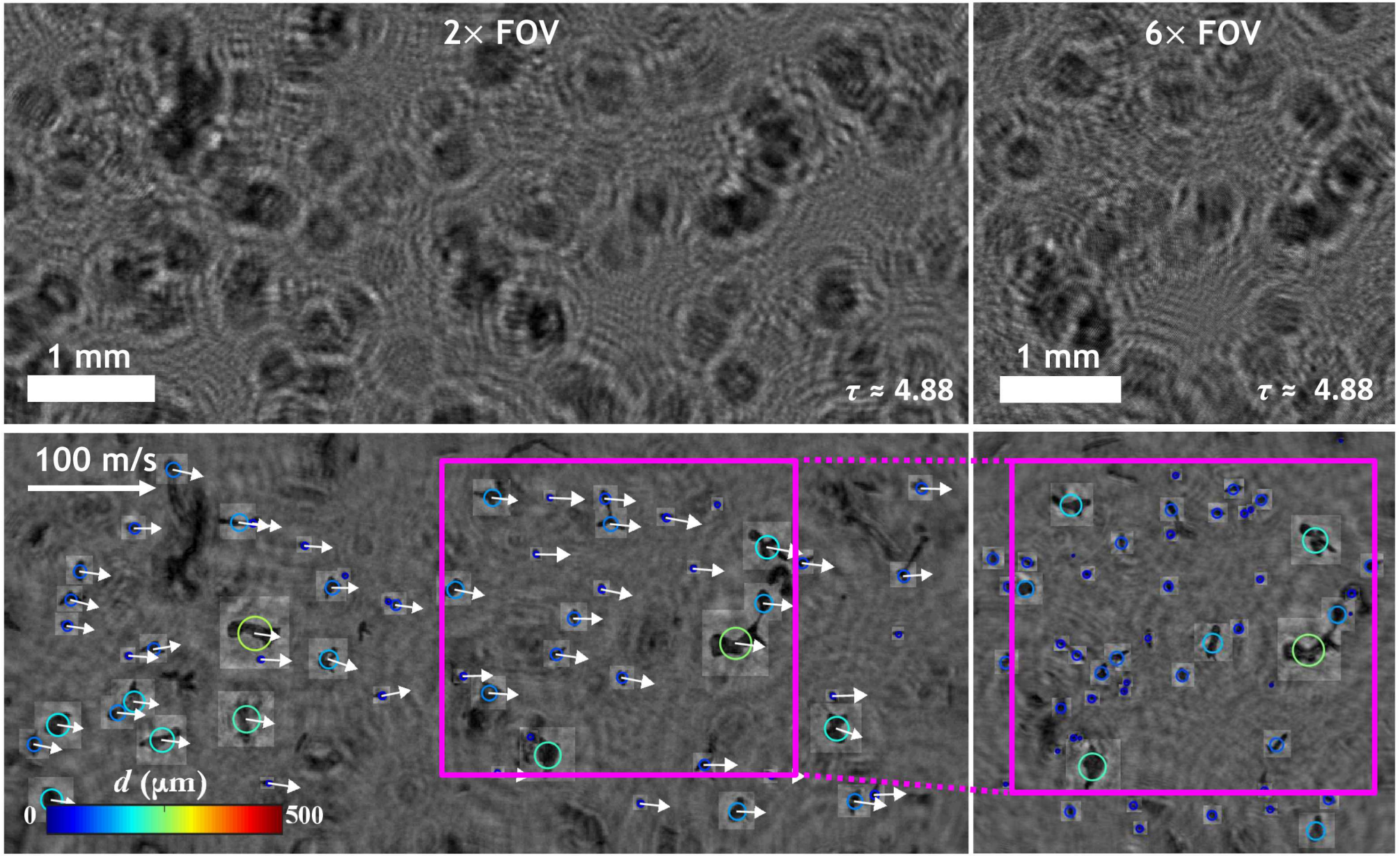

Digital In-line Holography of Droplets

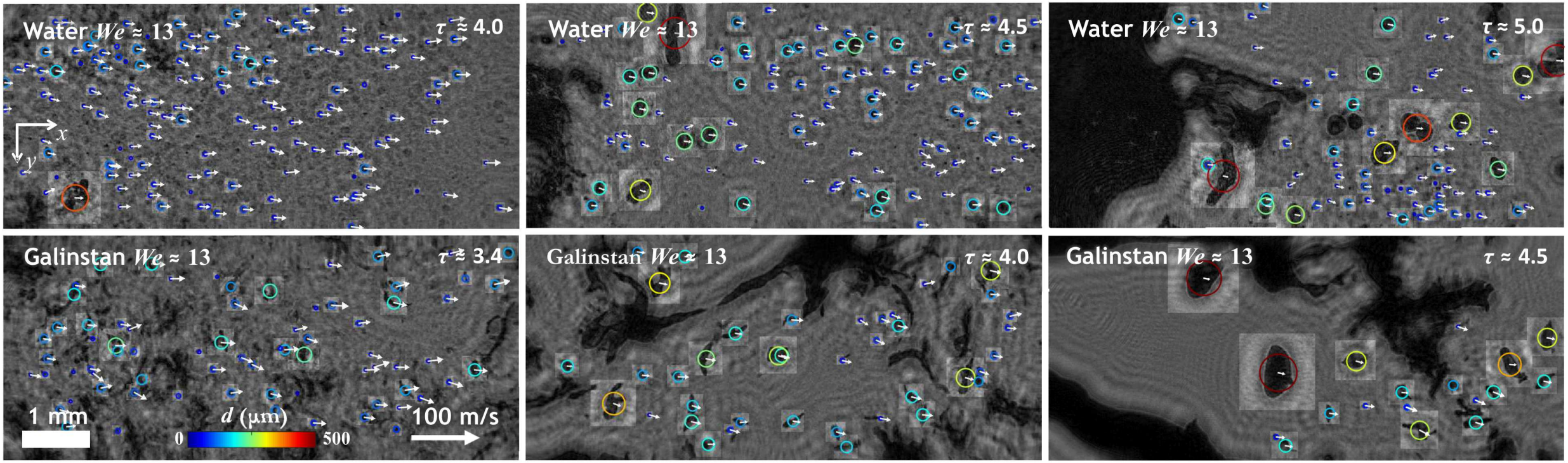

3D Droplet Distribution Reconstruction

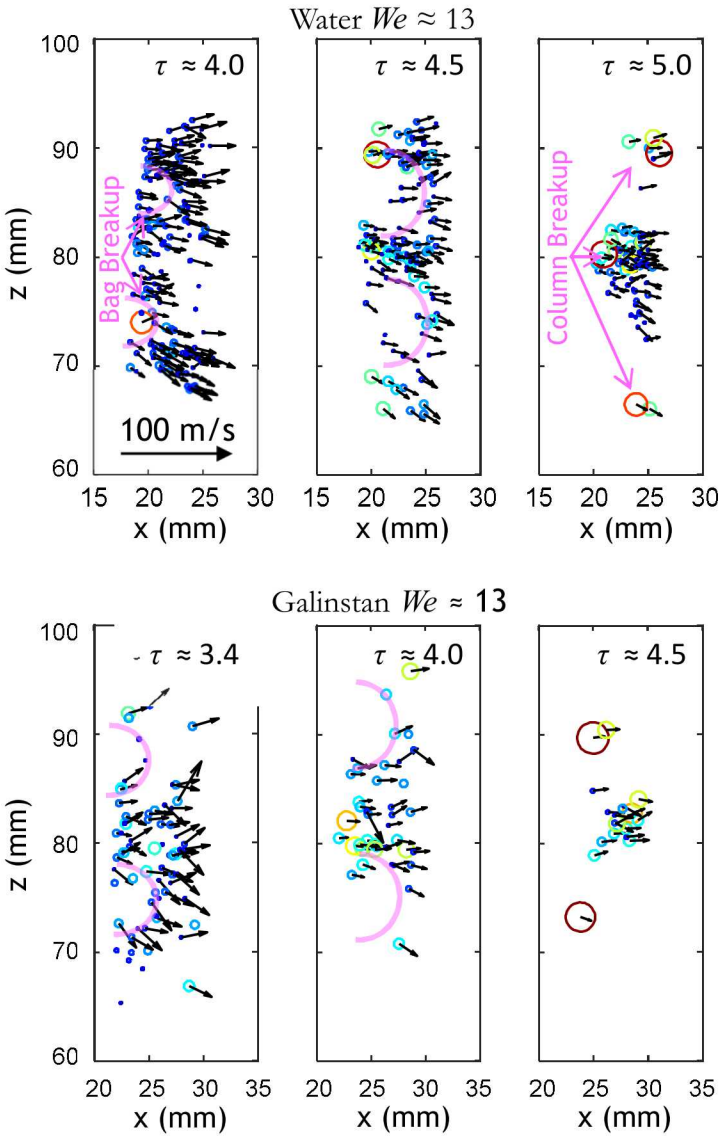

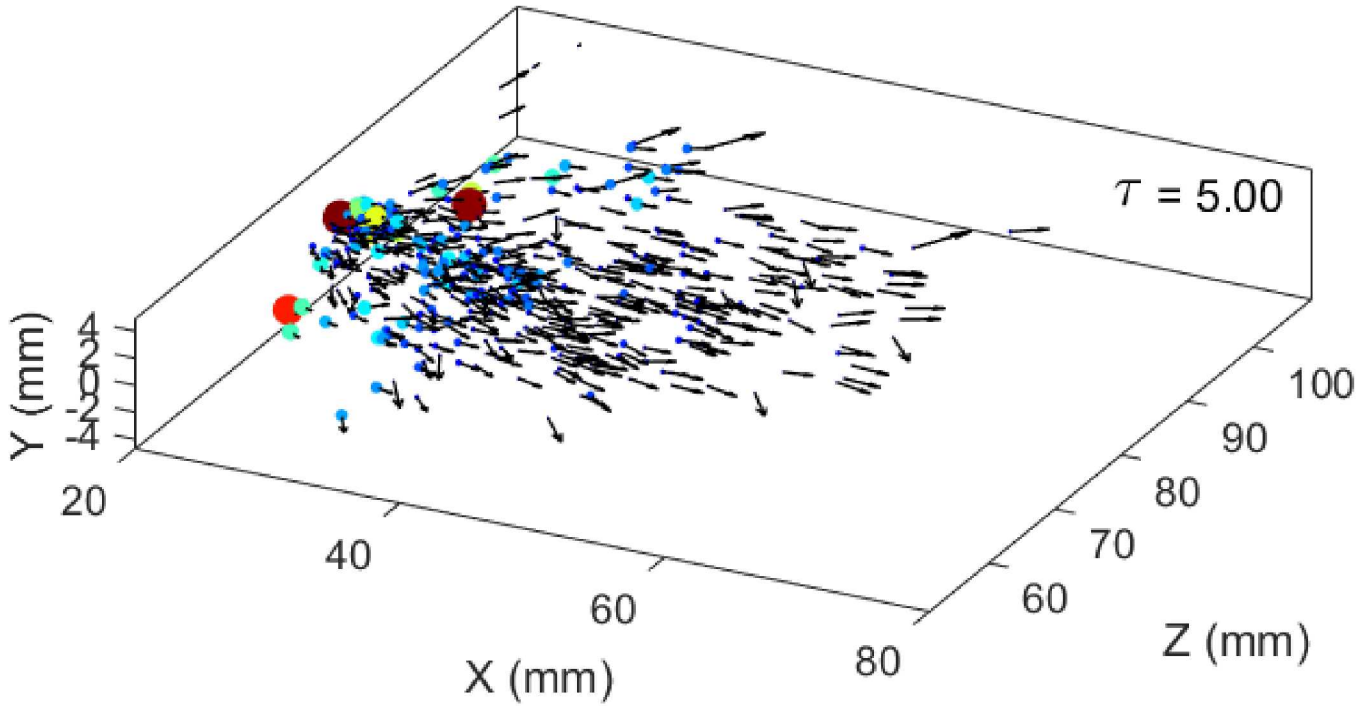

Diameter and Velocity

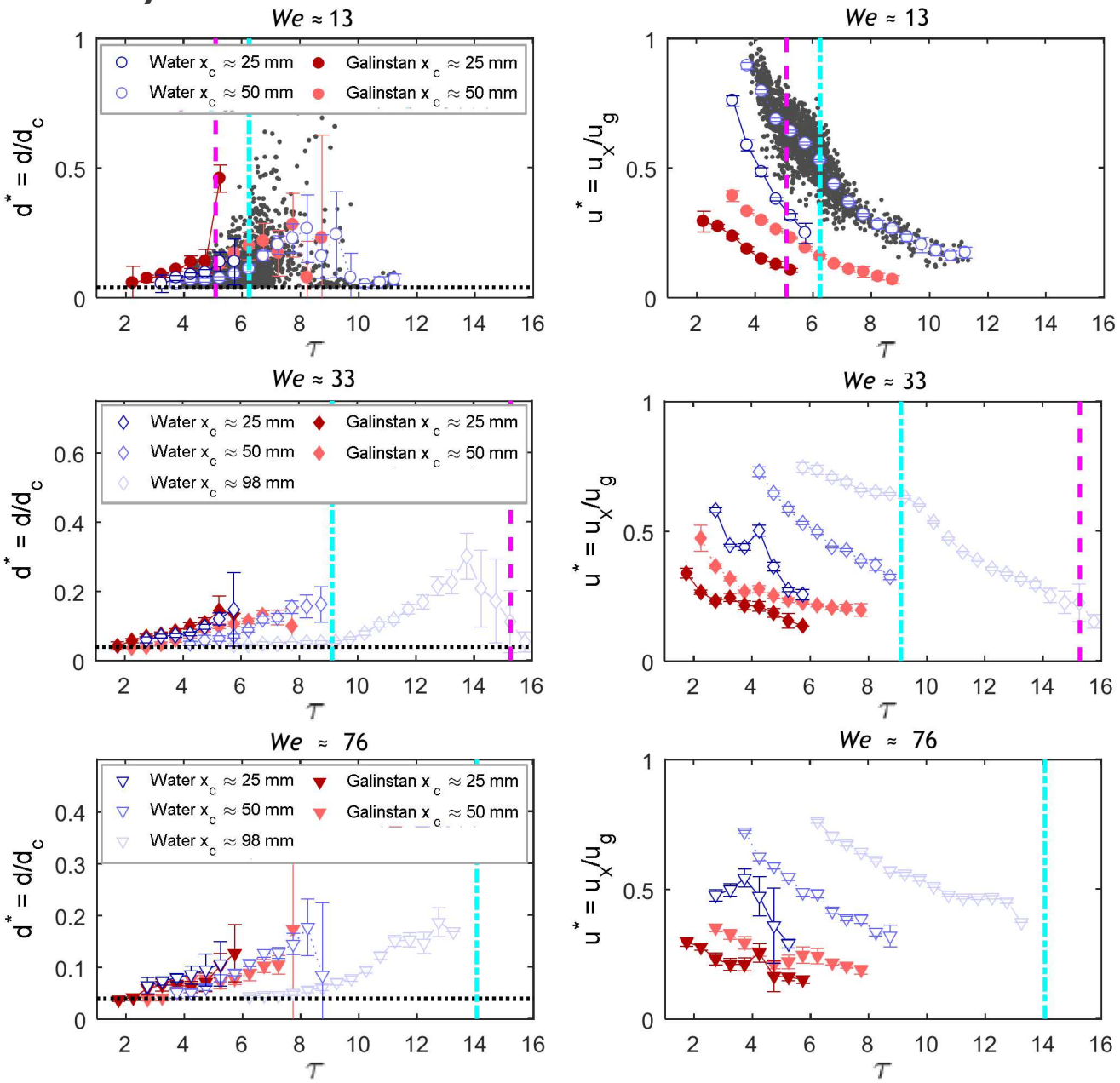

Probability Densities

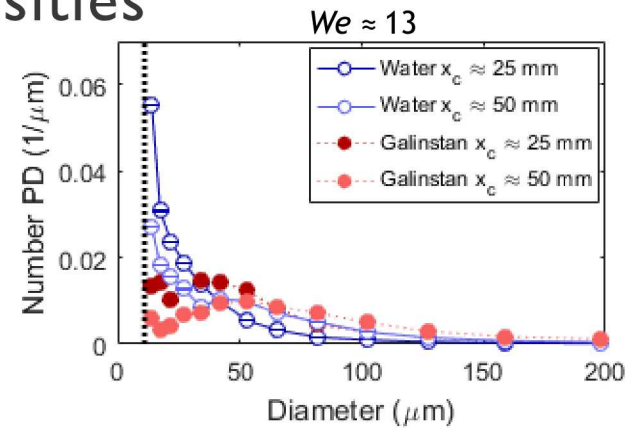

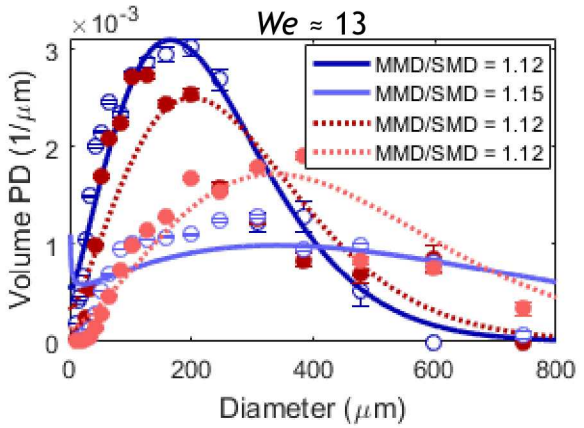

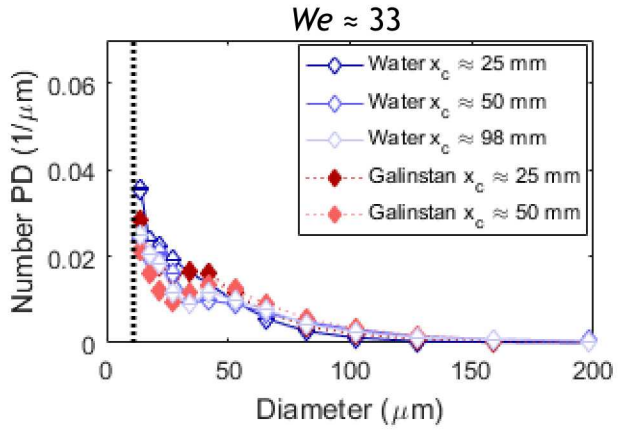

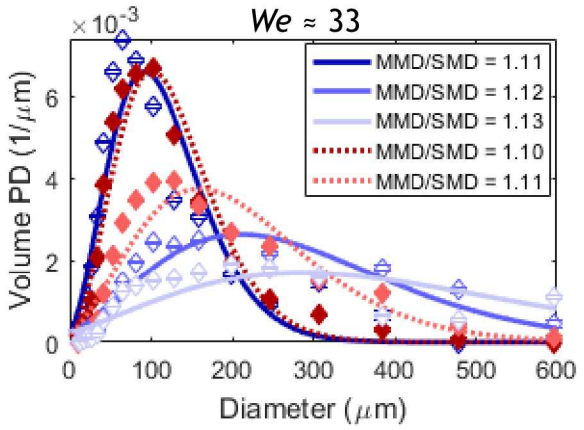

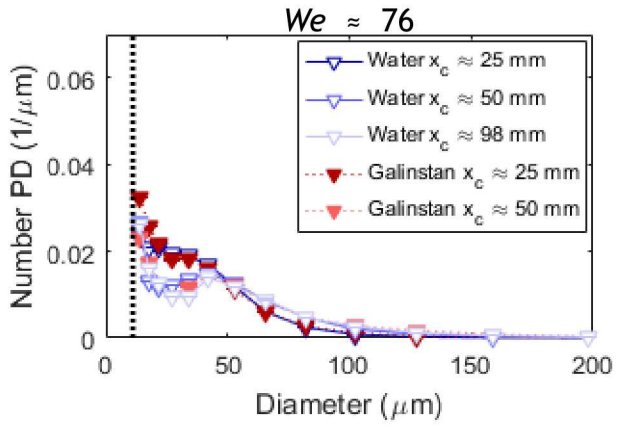

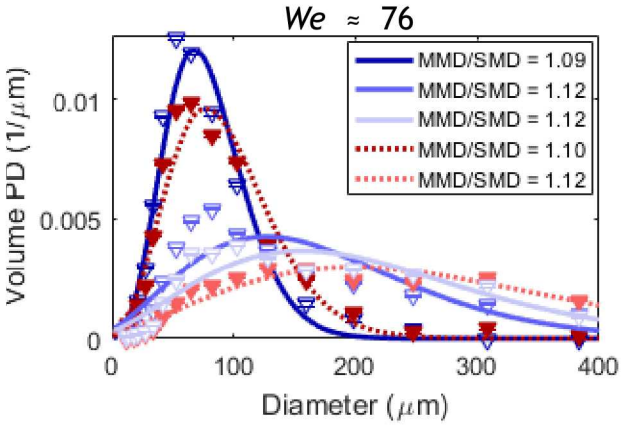

Size-velocity Correlation and Drop-Size Modeling